A STUDY OF THE VELOCITY FIELD IN M 82 AND ITS BEARING ON EXPLOSIVE PHENOMENA IN THAT GALAXY*

E. MARGARET BURBIDGE, G. R. BURBIDGE, and VERA C. RUBIN

University of California, San Diego

La Jolla, California

UNPUBLISHED PRELIMINARY DATA

Received May , 1964

*Contributions from the McDonald Observatory, University of Texas, No. 000.

ABSTRACT

21475

A detailed spectroscopic study of M 82 has been carried out from spectra taken in nine different position angles, and extending about 2' from the center of the galaxy (the radius of M 82 is about 4'). In many position angles, the velocity curves from the emission lines show steep gradients and large dips, when compared with the observed absorption line rotation curve obtained by Mayall, and confirm and give more information about the expansion stemming from an explosion as it was first discovered by Lynds and Sandage. It appears that the gas which was blown out forms a double cone with a half-angle $\approx 20°$. The true space velocity is about 450 km/sec for the gas furthest from the center whose line-of-sight velocity can be measured. The forms of the velocity curves in position angles 0° and 145° (the psotion angle of the major axis of the galaxy is 62°) show that we are observing gas in the exploded cones above and below the main body of the galaxy and these obey approximately linear velocity-distance relations, while the velocity curve of the gas in the main body of the galaxy indicates that it has undergone damping and deceleration. It is estimated that the explosion that gave rise to the gas now seen in the exploded double cone took place between 2 and 3 million years ago.

Study of the spectral features due to the stars in M 82 suggests that there is a real difference in stellar population between the central part and the outer parts.

Finally, a rediscussion of the energetics of the outburst is given. It is concluded that a total energy of $\sim 10^{57}$ ergs or greater may have been released in the last few million years, a value considerably greater than the minimum total energy obtained by Lynds and Sandage. This value has been obtained because it is assumed that the optical synchrotron radiation is produced by electrons with radiation half-lives that are short compared with the age of the primary explosion, so that many generations of electrons have been produced. A similar situation is thought to apply to the Crab and the jet in M 87, both of which are also sources of optical synchrotron radiation.

I. INTRODUCTION

Messier 82 is one of the most interesting of the nearby bright irregular galaxies. Many photographs of it have been reproduced and we may refer to those in the Hubble Atlas (Sandage 1961) as particularly good examples. Also, a series of remarkable plates have recently been published by Lynds and Sandage (1963). In Figures 1 and 2 we show two plates taken in blue light at the prime-focus of the 82-inch telescope which we shall use for reference.

The galaxy has been extensively observed spectroscopically by Mayall (1960) and the relation of its color to its spectral characteristics has been mentioned by Morgan and Mayall (1959). They concluded that the abnormally red color of the galaxy was due to the presence of large amounts of dust in it. The 21-cm studies (Volders and Högbom 1961) show that there is a large mass of neutral atomic hydrogen associated with M 82. The very large amount of uncondensed matter in the galaxy as manifested by the dust and the neutral atomic hydrogen suggest that it is comparatively young in evolutionary terms.

It was thought that a study of the inter-relation of the stars and the gas in this galaxy and also a study of its velocity field might give information on the physical conditions prevailing in a galaxy at a rather different evolutionary state from that of our own. Accordingly, an investigation using the nebular B-spectrograph attached to the 82-inch McDonald telescope was begun in 1960. Recently, one more spectrum was obtained with the prime-focus spectrograph on the Lick 120-inch telescope.

Before this material was analyzed the remarkable investigation of Lynds and Sandage (1963) based on filter photographs and spectra was published. In that paper they gave strong circumstantial evidence for supposing that about 1.5×10^6 years ago a violent explosion occurred in the central parts of M 82. In this outburst a large flux of relativistic particles was generated and

material was blown out in the direction of the poles. It appears probable that outbursts of this type occur in many types of galaxy (cf. Burbidge, Burbidge, and Sandage 1963). The input of energy, of magnitude $\geq 10^{56}$ ergs at least partly in the form of relativistic particles, means that much gas has been ionized and excited through the direct or indirect action of the particles, while the occurrence of an outburst suggests that probably the velocity field in the central parts may still have large components which were generated in the explosion.

II. THE OBSERVATIONS

Spectra were obtained with the slit in many position angles, and details of the observations are contained in Table 1. The slit orientations and the limits of the velocity measurements are marked on the plate in Figure 1. While the galaxy has an angular diameter of nearly 8', emitting gas can be detected only out to distances of about 1' from the center in the direction of the major axis. Thus the bulk of our measures, which come from the emission lines Hα, [N II] λλ6548, 6583, and [S II] λλ 6717, 6731, extend only over this region. In addition, emission lines of Hβ, Hγ, Hδ, [O III] λ 4959, λ 5007, [O II] λ 3727, and He I λ 5876 are visible in the central part, but were not measured. In the direction of the minor axis the Hα, [N II], and [S II] lines extend over the whole main body of the galaxy and Hα and [N II] extend also in the filamentary structure outside. In Figure 3 we show the red spectral region of six of the McDonald spectra. All of the measures obtained from the emission lines are given in Table 2, and, for all position angles except 46° and 57°.3, are plotted in Figures 4 - 11. For spectrum B 920, only absorption lines were measured, because on this long exposure the strong continuum obscures the emission lines.

Since there is no neat central nucleus in M 82, as there is in regular galaxies, we have some uncertainty in the locating of the slit in the various spectra. In setting the galaxy on the spectrograph slit for most of the McDonald spectra, the aim was to set the part appearing brightest to the eye, namely the H II region southwest of the dark lane, indicated in Figure 2, on the slit, in the hope that a reasonably strong continuum coming from this would be unmistakable on the resulting spectra, and that its center could be certainly judged. However, it is actually hard to judge the center of this region, as it is in fact part of a complex of H II regions. Different seeing conditions for the different spectra (although none were taken in poor seeing), coupled with a slight uncertainty in the guiding with the B-spectrograph, mean that one should judge by the light distribution in the resulting strip of continuum, as well as by its extent. Fortunately, in most of the spectra, other less intense strips of continua, coming from parts of the galaxy that appear optically bright in Figures 1 and 2, show up on the various spectra. We have measured the positions of the edges of such continua (which are good only to a few seconds of arc, because of lack of sharpness and the resolution of the photographic plate), and they are indicated in Figures 4 - 11 by the dark bands drawn along the horizontal axis. The shaded bands indicate regions of less strong continua. We have been guided by the positions of these edges, and also by the shapes of the velocity curves in adjacent position angles, in making small adjustments, up to a maximum of 4" (60 pc at the distance of M 82), in the position estimated during the measurement of the spectra as the zero of distance perpendicular to dispersion on the spectra. (The position estimated during measurement was either the geometrical center of the central strip of continuum or an estimate of its center of gravity where it appeared noticeably shaded.) In the rest of this paper, we denote by y the distance either from

the assumed center or from the point of crossing the major axis.

Bearing in mind this inherent uncertainty of order a few seconds of arc in locating the spectra, we show in Figure 1 the locations of the slit for all the spectra. For the two close to the minor axis which cross the major axis at a little distance from the center of the bright H II region, our location is consistent with the velocity occurring on the other spectra at the crossing-point (as will be seen below). In Figure 10, position angle 145°, we have plotted the velocities for position angles 155° (≡335°) and 142° (≡322°) read from the plot of Lynds and Sandage (1963), although their measures refer to positions displaced about 5" to 10" along the major axis from our spectrum. However, the agreement among the three sets of measurements is good.

It can be seen from Figures 4 - 9 that the central velocities given by each of these spectra that cross through an approximately common point show some scatter; they range from +280 km/sec (B 737) to +330 km/sec (B 720, 724). The mean value is +305 km/sec. Some part of the scatter is probably due to the slight uncertainty in location of the spectra described above, and some to small plate-to-plate errors.

III. ROTATION AND MASS

The fact that emitting gas can be detected only in the central parts of the galaxy means that measurements of the rotation of the bulk of the luminous matter must be made by using the stellar absorption lines. Dr. N. U. Mayall has very kindly given us his own original measures which come almost entirely from absorption lines, from four plates, with only a few velocities obtained from [O II] λ 3727. In Figure 4 we have replotted the mean points of Mayall, measured in position angle 62°, together with our emission line measures in the same position angle. We have not plotted our absorption-line measures in

position angle 62°, because Mayall's absorption-line data are much more extensive than our own, since we have been mainly concerned with the velocity field from the emission lines in the central region. Our absorption-line measures extend only from the center to y = 160" southeast; the mean values are listed in Table 3. For the outer part of the galaxy, (y < -60"), there is good agreement with Mayall's observations. For the region from the center to y - -40", our velocities are systematically lower than his. There is great scatter in the absorption line measures both in the raw data of Mayall and in our own results. The reasons for the scatter lie in the fact that the absorption lines are broad and difficult to measure against an often weak continuum. However, in view of the fact that we must suppose that the gas in the central parts of the galaxy has been excited and disturbed by the explosion, the absorption line measures alone must be used to determine the recession velocity of the center of mass of the system and also to define the rotation of the system as a whole.

In fitting the results of Mayall's rotation curve to those from our spectrum B 1197 in the same position angle, we have been able to examine a print of one of Mayall's spectra which he kindly loaned us, from which we could identify the various bright areas whose central measures provided his points. We have drawn a smooth curve through his points; it is shown in Figure 4. We find that this smooth curve crosses our zero axis at +300 km/sec, and this is in good agreement with the various central velocities read off our plots in other position angles passing through the same bright H II region which we have taken to be the zero point. From his measures, Mayall himself deduced the recession velocity for the center of the galaxy to be +275 ±40 km/sec (uncorrected for Galactic rotation, as are our plots in Figures 4 - 11 and the values in Table 2).

The recession velocity obtained from the 21-cm measures by Volders and Högbom is +190 km/sec. As they pointed out, this velocity is significantly different from the value obtained by Mayall which has been confirmed by our measures. Volders and Högbom have pointed out that agreement can be reached between the recession velocities obtained from the absorption line measures and the 21-cm line measures, if it is supposed that the true center is about 60" to the southwest of the apparent center (22 mm on Figure 2). From Figure 4 we see from Mayall's measurements that on the northeast side of the galaxy a maximum is reached in the rotation curve about 100" from the assumed center and that between 100" - 150" from the center the curve is falling off. Our absorption line measures confirm this maximum. However, on the southwest side, no corresponding minimum is observed in Mayall's observations. It might be expected that the underlying distribution of stars is symmetrical enough so that the rotation curve should show symmetry. If it were folded about the apparent zero in Figure 4, it would not be symmetrical, but if the true center were shifted to $\sim$ -30" on that plot and folded, greater symmetry would be achieved. Such a shift would imply that some of the mass is completely obscured on the southwest side of the galaxy. The apparent center which we have chosen has been deduced to be the center of mass because the stellar continuum is very strong here. However, there are wide variations in the strength of the continuum in this galaxy and these are obviously due to the presence of large amounts of obscuring matter and do not represent large local mass fluctuations. Thus there can be no obvious reason to suppose that in M 82 the center of mass and the center of light are coincident.

While these considerations can be used in support of the idea that the velocity of the center of mass is not well determined and that the 21-cm measures are to be preferred, it appears now that the interpretation of the

21-cm observations also can be questioned. Elvius (1964) has suggested that the H I regions in front of the strong central continuum radio source will absorb, rather than emit, the 21-cm line, thus distorting the 21-cm emission line profile from the galaxy. She has attempted to correct the profile on the assumption that this is occurring and has concluded that the recession velocity is $\sim$ +250 km/sec. This is in reasonably good agreement with the optical recession velocity which has been obtained by Mayall and ourselves.

Holmberg (1952) had earlier suggested that the recession velocity of M 82 obtained by Mayall was high when compared with the velocities of the other members of the M 81 group, and he suggested that the apparent center was not the true mass center and that a component of rotation was present. This argument suffers from the objection that there is no a priori reason for reducing the apparent velocity dispersion among the galaxies in the M 81 group. While it is true that it is M 82 which appears to have a velocity rather different from all of the other members of the group, it has been shown that such effects are present in other small groups (cf. Conference on the Instability of Systems of Galaxies, A. J., 66, 533, 1961). Further, there is always the possibility that M 82 is not at the same distance as M 81, but lies further away from us (see discussion in Section V).

Faced by all of these rather uncertain arguments, we have arbitrarily decided to base our discussion of the velocity field on the assumption that the apparent center is very close, or coincident with, the center assumed by Mayall. From Figure 4 we have concluded that the recession velocity at the center is about +300 km/sec. While this is slightly higher than the value quoted by Mayall, the difference is simply due to very small shifts in the position of the zero that was assumed by Mayall and by ourselves, and to the less steep curve which we have drawn across the center.

From the smooth rotation curve we can make a crude estimate of the mass of the galaxy, taking into account the many uncertainties involved. If we assume that the distance of M 82 is that of the M 81 group for which Lynds and Sandage (1963) give a modulus of 27.5, the distance is then 3.2 Mpc and at this distance 1" = 15.4 pc. If the smooth rotation curve drawn in Figure 4 is symmetrized by reading off velocities at equal distances on either side of the center and taking means, it reaches a maximum at ~110" from the center and then falls off very slowly out to ~150" from the center. A Keplerian mass estimate can be made by using the mean rotation velocity at ±150" of 136 km/sec. This gives

$$M_K = 1.0 \times 10^{10} M_\odot$$

where we have supposed that the plane of rotation is tilted at an angle of 8° 23' to the line of sight (Lynds and Sandage 1963).

A mass determined by supposing that there is a mass point at the center is always an overestimate. A second estimate can be made if it is supposed that the uniform spheroid approximation is to be preferred. This will reduce the mass to about $0.7 \times 10^{10} M_\odot$ for a reasonable value of c/a. An earlier estimate (Burbidge 1962[a]) was made on the basis of the same rotation curve by assuming that it is truly linear and by extrapolating it beyond 150" from the center to the end of the luminous extent of the galaxy. Thus a larger value of $1.5 \times 10^{10} M_\odot$ was obtained. The mass would also be increased over the values given above by supposing that the true center was displaced to the low-velocity side. In view of the many uncertainties associated with the central velocity which have been discussed earlier and the uncertainties in the geometry, we conclude that the mass is

$$1 \pm 0.5 \times 10^{10} M_\odot.$$

IV. THE VELOCITY FIELD IN THE GAS

We now turn to a discussion of the velocity field in the central region. It will be seen that the plots of our measures in Figures 4 - 11 show many asymmetries and irregularities. To attempt to investigate the non-circular motions in the gas the following procedure has been adopted. We have assumed that the stellar component of the galaxy is moving in purely circular orbits, and have therefore taken the smooth curve drawn through Mayall's observations in position angle 62° (Figure 4) to be the rotation curve of the galaxy. By folding this curve about the origin and forming a mean of the two sides, we have determined a mean rotation curve. We have then projected this curve into the various position angles of our observations, assuming the galaxy to be a flat disk, with the plane of the disk inclined 8° 23' to the line of sight. We have taken the center of the galaxy to be the bright H II region described above. We have then drawn smooth curves through the various plots in Figure 4 - 11, which delineate the gas velocity, and also through the plots in position angle 46° and 57°.3 which are not shown. Velocities were read off the smooth curves at intervals; the velocity zero on the horizontal axis on each curve was taken to be the central velocity appropriate to that spectrum (by this means correcting each for small systematic plate-to-plate errors). Figures 12 - 20 show these smooth curves and also the projected rotation curves, except that in position angle 155°, for which our measures extend over only a small distance. The differences between the observed and projected rotation curves in each case presumably indicate the non-circular gas velocities that are present. (If the true center of mass is displaced from the adopted center, the projected velocities will be affected by only very small amounts, but the point of intersection of the emission line curve and the projected rotation curve will be altered.) For position angles near the minor axis, 145° and 0°,

we have looked at a second model of the galaxy, a thick-disk galaxy, with a rotation curve which is independent of height above the plane, and at which we are looking as though it were the rim of a wheel. In position angle 0°, the resulting projected rotation curve is almost indistinguishable from that for the thin-disk model. In position angle 145° the projected rotation curves differ for each model and both are plotted in Figure 13.

In position angles 46°, 57°.3, 62°, 65°.5, and 69°, the nature of the departures of the gas velocity from the projected rotation curve is such that they may represent details of the rotation curve that are not discernible in the lower-resolution absorption-line measures. For instance, the steeper slope across the center and the humps are reminiscent of the central details in, e.g., M 31. On going further from the major axis, however, the departures show a systematic nature.

In position angles 30° and 83°, the humps and steep central slope are more pronounced. In position angle 145°, the line along which our observations lie did not pass through the "center" of the galaxy but crossed the major axis southwest of the center. This has been taken into account in projecting the rotation curve. This plot and that in position angle 0° (Figures 12 and 13) show departures that are predominantly negative, indicating velocities of approach with respect to the observer. Only at large distances from the center on the northwest side do positive velocities occur. This is in agreement with the general concept of an explosion; the galaxy is so optically thick in dust that we see only the near side until we go a great distance above the plane. The velocities reach ~ 200 km/sec in position angle 0°, and confirm the general run of velocities observed by Lynds and Sandage and by us in the direction of the minor axis. The details of the velocities outside the main body of the galaxy, as they relate to a model for the explosion, will be discussed in Section VI. Here we shall briefly consider the velocities within the main body.

All the curves except those in position angles 46° and 69° show an interesting feature, i.e., dips in velocity on either side of the central zero value, reaching minima about 20" - 30" or 300 - 450 pc from the center. The large bulk of gas and dust lying near the equatorial plane must have caused great damping and deceleration of the outward explosive pulse in directions close to this plane. In the brightest H II region (zero of the abscissae in Figures 4 - 9, 12, 14 - 20), the outward velocity has presumably been dissipated completely, perhaps leading to a transferral of kinetic to excitation energy that causes that gas to appear particularly bright, in both continuum and line radiation.

In position angle 83°, the big velocity minimum 18" southwest of the center occurs right in the very prominent dust lane (see Figure 1). Where there is prominent dust, there may be cooler temperatures and we should be looking less deep into the galaxy. On the explosion model, the gas at these positions would have greater outward velocities than gas closer to the center. An examination of Figures 6 - 9 indicates that this may be the case: there is a tendency for the dips (i.e., regions of more negative velocity) in the observed velocity curves to occur just where the observed continuum stops and the dust lanes begin. A similar phenomenon was observed in the observations of the radio galaxy NGC 5128 (Burbidge and Burbidge 1959), where large velocity fluctuations occurred in regions of the dark lanes.

There may be an analogy also with the characteristic dust lanes in barred spirals (Prendergast 1964). Here the dust lanes tend to be formed where Prendergast's computed models show discontinuities in the gas density, i.e., where there are shock fronts. In barred spirals, the dust may serve as a marker for regions of high density (if the rate of formation of dust depends on the gas density). Continuity of momentum across the front means that there

should be a discontinuity in velocity at the front. That shocks should propagate when we have non-circular velocities amounting to greater than 100 km/sec, is obvious. Although we have not measured any abrupt discontinuities in velocity in M 82, these could be present, and there may also be fine structure in the velocity field, which we cannot resolve on our spectra. The considerable breadths of the emission lines of Hα and [N II] in our Lick spectrogram, which was taken in not particularly good seeing (i.e., the seeing disk was about $2\frac{1}{2}$ seconds of arc), support the possibility of fine structure in the velocity field.

V. STELLAR POPULATION OF M 82

In earlier papers we have commented that the stellar component in M 82 showed differences in stellar population from one part of the galaxy to another (Burbidge 1962b, Burbidge and Burbidge 1962). In part, we arrived at this conclusion from observation of the abrupt switch from an emission-line spectrum near the center to an absorption-line one further out; across this dividing line the general appearance of the galaxy on blue photographs shows no real change; in particular, the amount of dust in emission-line and absorption-line regions appeared about the same. This suggested to us that the amount of material uncondensed into stars was the same and that the only difference might be that in one region the gas was ionized and was excited into H II regions, and in the adjacent region it was not. We interpreted this to be due to the presence of unseen massive O and B stars near the center and their absence elsewhere. Now it is clear from the work of Lynds and Sandage (see particularly their photographs in Hα light) that the abrupt change from an ionized to an unionized region is due to the supply of energy from the explosion in the former and its dissipation in the uncondensed material, until at a certain distance from the seat of the explosion the energy supply is insufficient

to ionize the hydrogen.

However, the differences in absorption-line spectra which we noted in 1961 have still to be accounted for. On our spectrum with the longest exposure, B 920, running from the center to the northeast end of the galaxy, we find a spectral type of A2-5 to be characteristic of the extended bright area running from 25" to 65" northeast of the center. We cannot be more precise than this, as our spectrum in the photographic region had a dispersion of only 400 A/mm, but this is in agreement with Humason's quoted type of A5 (Humason, Mayall, and Sandage 1956). However, even on this dispersion it is plain that in the bright area 100" to 130" northeast of the center (i.e., just beyond the strong dust bars about 70" from the center) the spectral type is later. The H and K lines of Ca II are stonger with respect to the hydrogen lines, and the G band is clearly seen. A type around F 0 - F 2 is more appropriate here. It might be thought that a systematic difference could arise in judging spectral type in these two regions on one spectrum because the region nearer the center is brighter and hence more intensely exposed. However, we have made a careful comparison of this strip on the shorter-exposure spectrum B 1197 with the further-out strip on B 920; it happens that the photographic density of the two regions is about the same on these two spectra, and the difference in integrated spectral type seems to be real.

This implies that more massive stars, further up the main sequence, are present in the stellar population closer to the center of the galaxy than further out, a surprising result. The absence of resolved stars (which are seen in M 81 and, according to Sandage, not in M 82) is a further puzzle. Usually the presence of large quantities of dust in a galaxy is closely correlated with the existence of young, massive O and B stars in association with it (Baade 1950). Although the input of kinetic energy into the uncondensed material of M 82 may well affect the conditions for star formation, this should not, if the

explosion occurred only a few million years ago, have a noticeable effect on the present stellar luminosity function except for the most massive O and B stars; late type supergiants and A supergiants should still be present.

It is possible that the recent explosion is not the only outburst that has occurred in M 82. The physical connection between the dust which is often a prominent feature of radio galaxies and the radio emission is a long-standing puzzle (cf. Burbidge and Burbidge 1964). It is possible that quantities of dust are produced in explosive events, but that the dust clouds cannot serve as seats of star formation until their kinetic energy has been dissipated.

The absence of resolved stars in M 82 might be due to its being further away than M 81, and physically unconnected with it. This would provide an explanation for the velocity difference between M 81 and M 82, discussed in Section III. However, one of the other members of the M 81 group, NGC 3077, is an irregular containing much dust and having a strong emission-line spectrum; it bears some resemblance to M 82. It would be a strange coincidence if these two objects were physically unconnected and only by chance lie in the same area of the sky. We think it more likely that M 82 is a part of the M 81 group, so that the absence of resolved stars in it has to be a result of its nature.

VI. INTERPRETATION OF VELOCITY FIELD; TIME SCALE ASSOCIATED WITH THE PRIMARY OUTBURST

We now consider the bearing of these results on current ideas concerning the state of M 82 stemming from the work of Lynds and Sandage. These authors concluded that the explosion took place 1.5×10^6 years ago; this time was derived by supposing that the expansion caused by the explosion followed a linear velocity-distance relation between the line-of-sight velocity and the plane-of-the-sky distance. Our study of the velocity field in the direction of the minor axis, which is best shown by Figures 5, 10, 12, and 13, shows that a linear

approximation to the velocity-distance relation is too coarse. The curves show that there are considerable irregularities in the velocity-distance relation within the main body of the galaxy, but that if a straight line is drawn through these velocities, the slope is much smaller than that derived by Lynds and Sandage by approximating the whole run of velocity by a linear relation, while the slope outside the main body is steeper than their average. The orientation of M 82 was derived by Lynds and Sandage from the axial ratio, by assuming the galaxy to have an intrinsic axial ratio of 1/10. Any assumption that the true axial ratio is larger than 1/10 gives smaller values of the angle between line of sight and principal plane, and the true axial ratio can hardly be smaller than 1/10 (if the galaxy were an infinitely thin disk, the angle would be 10°).

On the assumption that the ejection has taken place only in a direction perpendicular to the principal plane of the galaxy, the correction factors for turning projected distance d' into true distance d, and line-of-sight velocity v' into true velocity v are $d = 1.01\ d'$ and $v = 6.86\ v'$. These are the factors which were used by Lynds and Sandage in deriving the time scale of the explosion from a linear velocity-distance relation. Since the largest apparent ejection velocities which we see are ~ 230 km/sec, this would imply that the furthest material is moving with a true velocity of about 1500 km/sec.

However, our observations suggest that this simple picture of gas streaming out only in a direction perpendicular to the principal plane cannot be correct. The reasons for this are as follows: Firstly, spectroscopic observations at great distances from the principal plane in the position angles 145° and 0° show strong Hα and [N II] emission which certainly is associated with the explosion. Hence, the gas must be distributed over a cone of half-angle of at least 20°, with the vertex near the center of the galaxy. The Hα photographs of Lynds and Sandage confirm the presence of gas in a roughly cone-shaped region.

Secondly, if the gas velocity is only along the minor axis, then in position angles 145° and 0° at great distances from the plane, large negative velocities (with respect to the center) would be observed on the south side where the minor axis is tilted toward the observer, and equally large positive velocities would be seen on the north side. However, no large positive velocities are seen. In position angle 145° the velocities are negative to a distance of 80" from the origin.

As an alternative model we therefore propose that the region containing the filaments is a solid double cone of half-angle about 20°, with the axis of the cone approximately along the minor axis of M 82. We shall actually adopt position angle 160° which is mid-way between 140° and 0°, as the major axis of the cone. The vertex of the cone is in the general region of the center of the galaxy but it cannot be determined precisely. We assume that the cone is optically thick enough in the line radiation so that we do not see more than the front layers. Because the minor axis of M 82 is inclined at about 8° to the plane of the sky, the conical region filled by the filaments will extend (20° -8°) or 12° toward the observer on the north side of the galaxy, where the minor axis is pointing away, and (20° +8°) or 28° toward the observer on the south side of the galaxy. This model is sketched in Figure 21. At the greatest distances from the center, the fastest moving material is moving more or less along the axis of the cone.

We now examine the velocities which would result from such a model. We assume that the gas is moving radially from the origin with true velocities v (r) which are similar in the north and the south parts of the cone. Then, in the south, the observed line-of-sight velocities, v' (r), will be the filament velocity projected through the angle (90° - 12°). Hence we may write:

$$v'(r)_{north} \text{ cosec } 12^\circ = v'(r)_{south} \text{ cosec } 28^\circ.$$

Thus on this model, the line-of-sight velocity for the filaments on the south side should be about twice the line-of-sight velocity of the filaments on the north just because of the orientation of the cone and the observer.

We now examine the velocities in position angle 0°. At 90" north of the origin, the velocities are positive coming from gas at A (Figure 21). At B(-80") the observed line-of-sight velocity is zero, and at C(-70") it has decreased to about -40 km/sec. The observed velocity then is approximately constant at this negative value until it rises sharply at about -20". This point corresponds to D, where the gas in the principal plane of the galaxy is obscuring the cone. At the origin E the observed velocity is zero. From the origin toward the south, the velocities decrease sharply as the observed velocities come from the foreground cone, which is obscuring the disk of the galaxy. Material with greater velocity is observed at a greater distance from the site of the initial disturbance.

In the regions between -20" and -60", and between +20" and +60", the observed velocities come from the near sides of the cone. The velocities observed on the south are about 3 times larger than those observed on the north side, in good agreement with the model. At the extreme north, where the observed positive velocities may come from gas moving along the minor axis, we may compute the true velocity of the gas:

$$v \ (y = -70") = 65 \text{ cosec } 8^\circ = 470 \text{ km/sec.}$$

If we suppose that the corresponding observations of the south come from the foreground cone then

$$v \ (y = +70") = 200 \text{ cosec } 28^\circ = 430 \text{ km/sec.}$$

Even from these very general arguments it seems clear that the cone occupied by the filaments cannot have a half-angle in the direction of the observer that is much greater than 20°, for then the velocities north of the nucleus would be more negative, almost as negative as those on the south side. It is possible, however, that the filaments could occupy a fan-shaped region, with an angular extent across the line-of-sight greater than the 20° in the line-of-sight. However, such a model would not alter the conclusions reached here.

Using this model we can now attempt to derive a new time scale for the first explosion in the galaxy. The form of the expansion curves which are shown best in Figures 12 and 13 is now interpreted as follows: The part of the curve between $\sim \pm 30"$ from the center represents motions in the main body of the galaxy (perhaps remnants of the expansion which have suffered large decelerations) while the linear parts of the curve beyond +30" and -30" show expansion in the cones both above and below the main body of the galaxy. These can roughly be represented by relations of the form

$$d\,(v) = kv$$

where d is the true distance of a part of a filamentary structure from the center of expansion and v is the true space velocity of this filament. Since a roughly linear relation is obeyed it is clear that deceleration in this region can be neglected. From Figures 12 and 13 we see that in that part of the cone projected in front of the galaxy, i.e., on the negative velocity side, the apparent slope of the linear part of the curve is about 4 km/sec per second of arc.

Our interpretation of the curves implies that at distances $\geq$ 30" from the center the products of the explosion move out from the "surface" of the galaxy. From the site of the explosion out to this point deceleration has been due both

to gravitational effects and to interaction with uncondensed material. A point on the surface can then be considered as the origin of the further expansion. The total time since the explosion is then given by

$$T = (t + k^{-1})$$

where t is the time taken for the fastest material to travel from the explosion center to the "surface" of the galaxy.

We first derive k. We shall consider only the material in the cone tilted toward us (on the negative side) since it has been shown above that the geometry of this model derived by considering motions above and below the plane is satisfactory. Then since

$$d = d' \sec 28^\circ = 1.13\, d',$$

$$v = v' \operatorname{cosec} 28^\circ = 2.13\, v',$$

$$k = \frac{10^6 \times 8.17}{x} \text{ years},$$

where the slope of a linear relation is x km/sec per second of arc. For $x = 4$, $k = 2 \times 10^6$ years.

To make an estimate of t is more difficult. It is clear that there must have been a tremendous amount of deceleration of the material as it passed through the disk of the galaxy. However, strictly speaking, we can only make an estimate of an upper limit for t based on the true space velocity of the furthest out (and fastest moving) gas which is seen. This, with the geometry we have used, is about 450 km/sec. Thus, an upper limit on this time t is the time to traverse about 450 pc at 450 km/sec which is $\sim 10^6$ years. Thus

$$T = (t + k^{-1}) < 3 \times 10^6 \text{ years}.$$

If gas very much further out is detected the value of T must be reduced. Our conclusion, based on this model, is that

$$2 \times 10^6 < T < 3 \times 10^6 \text{ years}.$$

If we returned to the assumptions of Lynds and Sandage, the corresponding age would be $0.6 \times 10^6 < T < 1 \times 10^6$ years. However, we have explained earlier that this latter model is inconsistent with our observations. It should be stressed that on our interpretation of the observations we are looking only at the front surfaces of the cone of exploded gas. It is difficult to understand how this could be true unless there were a tremendous amount of dust embedded in the gas and part of the ejected material. It is reasonable to suppose that this is the case because much dust must have been ejected from the plane.

VII. ENERGETICS OF THE EXPLOSION (S)

Clear evidence exists that an outburst took place in M 82 between 2 and 3×10^6 years ago. It is possible that outbursts with much shorter characteristic time scales have taken place in the intervening period and are still taking place at the present time. However, the evidence for this is ambiguous or indirect and it is related closely to consideration of the energetics of the galaxy as a whole. We shall attempt now to discuss some aspects of these energetics.

As was pointed out earlier, there are irregularities in the velocity curves which are associated with the central region of the galaxy and which have characteristic sizes of about 50 km/sec and scales of about 100 pc. Such scales would imply times $\sim 2 \times 10^6$ years, so they still could be remnant motions associated with one outburst which blew material out to great distances from the plane, though they might also be decelerated motions associated with later explosions.

The ionized gas which cools through emission of Hα and the forbidden lines of [N II] and [O II] has a characteristic cooling time of 10^3 - 10^4 years. Consequently it must be continuously reheated. Lynds and Sandage have suggested that this must take place through absorption of synchrotron radiation from

beyond the Lyman limit. A second process which may also be important is collisional excitation due to a flux of low energy particles (Burbidge, Gould, and Pottasch 1963). Both of these processes require the presence of fluxes of particles which either must have lifetimes $\gtrsim 2 - 3 \times 10^6$ years and thus have originated in the first outburst, or else must have been re-accelerated or produced in later outbursts.

We now consider in more detail the flux of relativistic particles in M 82. The galaxy is a weak synchrotron source by virture of its radio emission and Lynds and Sandage argued that the polarization of the optical continuum radiation observed by Elvius and Hall indicates that it is a strong optical synchrotron source. However, Mrs. Elvius (1962) suggested that the polarization might well be due to scattering by the dust. More recently Sandage and Miller (1964) have shown that an exceedingly high degree of polarization is present in the continuum radiation from filaments near to the main body of the galaxy and such a large amount of polarization (> 50%) gives conclusive proof that it is synchrotron radiation. The following discussion of the energetics of the explosive mechanism in M 82 depends on our accepting the view that a large part of the optical continuum flux is synchrotron radiation.

The total energy in the electrons which is required to explain the synchrotron flux has been calculated by Sandage and Lynds. It is

$$E_R = 3.36 \times 10^{47} H^{-3/2} \text{ ergs},$$

and the total energy in the magnetic field is

$$E_M = 9.1 \times 10^{63} H^2.$$

Following a suggestion of Spitzer, Lynds and Sandage obtained an estimate of the total energy in the particles, by assuming that the electrons had half-lives against radiation such that

$$t_{\frac{1}{2}} \geq T,$$

where T is the age of the explosion. The philosophy behind this approach is that it attempts above all to minimize the energy requirements by ignoring the possible presence of a proton flux, and by supposing that the electrons which were produced in a single outburst are still able to radiate the observed fluxes of optical and radio radiation. Since

$$t_{\frac{1}{2}} = \frac{8.35 \times 10^{-3}}{H_{\perp}^2 E} \text{ years}$$

where E is measured in Bev and

$$\nu_c = 1.61 \times 10^{13} H_{\perp} E^2 \text{ c/s},$$

this means that, for the optical synchrotron radiation, ($\nu_c \approx 6 \times 10^{14}$ c/s) $E = 5.4 \times 10^{12}$ ev and $H_{\perp} = 1.2 \times 10^{-6}$ gauss. Then the total energies in particles and field are

$$E_R = 2.6 \times 10^{56} \text{ ergs}$$

and

$$E_M = 1.3 \times 10^{52} \text{ ergs}.$$

Thus the bulk of the energy of the explosion has been released in the form of kinetic energy of gas and ultra-relativistic electrons (even the lowest-energy electrons responsible for radio radiation at 100 Mc have energies of $\sim$5 Bev). A negligible fraction is contained in magnetic field energy. In the other two optical synchrotron sources which are known, the Crab Nebula (Oort and Walraven 1956, Woltjer 1958, Burbidge 1958) and the jet in M 87 (Shklovsky 1955, Burbidge 1956) rather different conditions are thought to prevail. In the Crab a number of arguments have led to the conlusion that the magnetic field has a strength somewhere in the range 5×10^{-4} - 10^{-2} gauss so that the half-lives of the range 40,000 - 50 years are involved. In each of these cases it is clear that the time scales for the decay of the optical electrons are much shorter than the time scales associated with the explosive phenomena as they can be

derived from optical and radio astronomical arguments. Thus it has been concluded that in these cases there must be a continuing generation of electrons either through re-acceleration processes or by successive outbursts. This point of view has been taken for M 87 by Shklovsky and more generally by Burbidge, Burbidge, and Sandage (1963).

We believe that such conditions of continuous activity are probably also present in M 82. As an example of different energy conditions which are compatible with the observations we consider a situation in which it is supposed that there is equipartition between the magnetic energy and particle energy. It is unreasonable to suppose that there is no proton flux, so let us suppose that the total energy in the protons is just equal to that in the electrons. Then we find that the total energy in particles and magnetic field is about 10^{55} ergs and the half-lives of the optical electrons are about 10^{4} years. In this case, at least 200 generations of electrons must have been produced. This would imply that the total energy which has been generated in the particles is at least 10^{57} ergs.

The division in energy between protons and electrons depends closely on the initial conditions in which the particles are produced. If protons and electrons are injected initially with non-relativistic energies and are accelerated in a Fermi-type process it is very hard to avoid the conclusion that the energy in the proton flux must exceed that in the electron flux after the acceleration is complete. The loss processes are through nuclear collisions and escape for the proton flux, and through synchrotron loss for the electron flux. Since synchrotron loss is a much more powerful mechanism of energy loss for an electron than nuclear collision is for a proton, the proton-electron energy ratio must increase unless the escape times of the protons are comparable with the synchrotron half-lives of the electrons.*

*The half-life of a 1000 Bev electron moving in a field of 10^{-5} gauss is 8×10^4 years, while the mean life of a proton with the same energy against nuclear collision in a gas of density 1 atom/cm^3 is about 3×10^7 years. If a proton is to escape in a time comparable with the half-life against radiation of the electron, then it must travel a distance of only about 25 kpc to escape.

Thus as far as total energy in the outburst is concerned this mechanism of production of particles (injection at non-relativistic energies followed by Fermi acceleration) seems to imply that far more energy was gained and retained by the protons. Whether they are still present in the galaxy is another question.

To minimize the energy in the particles to about 2×10^{56} ergs as was done by Lynds and Sandage would seem to imply that they were injected in an initial explosion or in a series of outbursts already at relativistic energies and by a process that discriminates against protons. This would mean that equal numbers of positrons and electrons were injected to maintain charge conservation. The only process which has been proposed which might give rise to such effects involves the gravitational collapse of a large mass and the injection of particles at very high initial energies corresponding to the Fermi levels at excessively high densities ($> 10^{30}$ gm/cm^3) (cf. Hoyle and Narlikar 1964; Hoyle, Fowler, Burbidge, and Burbidge 1964). Even under these conditions we would not expect to get highly efficient acceleration to these levels but would propose rather that somewhat lower energy fermions are produced so that again many generations and continuous activity would be involved.

In any of these revised models the total energy input in the last 2×10^6 years must be considerably higher than the minimum obtained on the assumption that only a single outburst occurred. The minimum energy in particles, if we suppose that multiple outbursts are involved, is probably about 10^{57} ergs and larger values are entirely possible. On the other hand,

the kinetic energy of the filamentary structure was estimated by Lynds and Sandage to be about 2.4×10^{55} ergs. The geometrical model which we have used would reduce this because the true space velocities in our model are lower. The reduction in the kinetic energy of the filaments is practically a factor of 10. However, we believe that much dust has been ejected in the explosion so that the kinetic energy of the ejected matter may still be close to 10^{55} ergs.

The large scale alignment of the magnetic field required to explain the very high degree of optical polarization recently discovered by Sandage and Miller might be difficult to explain in a situation in which we have approximate equipartition between magnetic flux, electron flux present now, and kinetic energy of the exploding material. However, this may be attributed to an over-bearing flux of protons with local energy densities high compared to the other energy modes which in continuous processes of generation have "straightened" the magnetic flux lines as they have streamed out.

In conclusion, it is of some interest to consider briefly the source of material which has been blown out of the plane of the galaxy. Volders and Högbom concluded that the mass of neutral atomic hydrogen in M 82 amounted to

$$M_{AH} = (1.1 \pm 0.2) \times 10^{9} M_{\odot}$$

for the distance they chose. For the distance we have used here this is increased to $1.6 \pm 0.3 \times 10^{9} M_{\odot}$. If the total mass of the galaxy is $10^{10} M_{\odot}$ this means about 16% of that mass is in the form of atomic hydrogen. While dust is very obviously present, it cannot contribute very much mass since it can be formed only out of the heavier elements. Thus we may suppose that $M_D \leq 0.01 M_{AH}$ unless the composition of the uncondensed material is very different from normal. The mass of molecular hydrogen is uncertain. It may be comparable with the atomic hydrogen. In any case the large amount of gas implies that the mean density of interstellar matter in the galaxy is high.

If we suppose that it can be approximated by a uniform spheroid of axial ratio 1/10, then the total volume is about 5×10^{65} cm^3 and the mean density of uncondensed matter is $\gtrsim 6 \times 10^{-24}$ gm/cm^3. Some mass concentrations must have been present toward the center so that we might suppose that the mean density in the region of the primary explosion was originally $\gtrsim 10^{-23}$ gm/cm^3. A spherically symmetrical explosion must then have given rise to a shock which was propagated outward and passed through a total mass $\gtrsim 2.5 \times 10^{8}$ $M_\odot$ of gas and dust before material was ejected from the "surface" of the galaxy in the direction of the axis of the cone described earlier. The total amount of gas which has been ejected is $\sim 10^{6}$ $M_\odot$, according to Lynds and Sandage. In the main body of the galaxy the gas has been excited out to distances $\sim$ 900 pc from the center in the direction of the major axis so that the explosion, or explosions, has been violent enough to excite some 4×10^{7} - 7×10^{7} $M_\odot$ of gas and dust. Further progress in understanding the energetics of explosions of this type may be achieved when detailed calculations of the propagation of strong shocks from a central outburst on the galactic scale are undertaken.

The major objection to a modification of the energetics along the lines proposed earlier in this section may be thought to lie in our refusal to accept the most "conservative" model as the most probable one. Our reasons for this, apart from those discussed above, stem from the belief that the activity in M 82 is yet another manifestation of the generation of vast fluxes of energy by processes which are not yet properly understood and which in many cases demand minimum energies in excess of 10^{60} ergs. This situation has been summarized elsewhere (Burbidge, Burbidge, and Sandage 1963). While the scales of the processes may cover a wide range we believe that many different manifestations of the outbursts (strong or weak radio characteristics, Seyfert characteristics, optical synchrotron radiation) often arise because the explosions take place

in different environments (elliptical, spiral, irregular, or recently forming, galaxies) and they are observed at different stages in their evolution. Thus we might well expect that we may not detect the release of a large part of the energy in many cases.

We wish to thank Dr. N. U. Mayall for giving us access to his spectroscopic material on M 82 and Dr. Joan Crampin for computational assistance. We also wish to acknowledge helpful discussions with Drs. K. H. Prendergast, Allan R. Sandage, and C. R. Lynds.

This work has been supported partly through a grant from the National Science Foundation and partly by NASA through Grant NsG-357.

REFERENCES

Baade, W. 1950, Pub. Michigan Obs., 10 7.

Burbidge, E. M. 1962a, Trans. I.A.U., 11B (London and New York: Academic Press), p. 306.

_____ 1962b, "The Distribution and Motions of Interstellar Matter in Galaxies" (New York: Benjamin), p. 123.

Burbidge, G. R. 1956, Ap. J., 124, 416.

_____ 1958, Ap. J., 127, 48.

Burbidge, E. M. and Burbidge, G. R. 1959, Ap. J., 129, 271.

_____ 1962, Ap. J., 135, 694.

_____ 1964, Proceedings of the Dallas Conference, in press.

Burbidge, G. R., Burbidge, E. M., and Sandage, A. R. 1963, Rev. Mod. Phys., 35, 947.

Elvius, A. 1962, Lowell Obs. Bull., 5, 281.

_____ 1964, Nature, 201, 171.

Holmberg, E. 1952, Medd. Lund Astron. Obs., Series I. No. 180.

Hoyle, F., and Narlikar, J. V. 1964, Proc. Roy. Soc., in the press.

Hoyle, F., Fowler, W. A., Burbidge, G. R., and Burbidge, E. M. 1964, Ap. J., 139, 000.

Lynds, C. R., and Sandage, A. R. 1963, Ap. J., 137, 1005.

Mayall, N. U. 1960, Ann. d'Ap., 23, 344.

Morgan, W. W., and Mayall, N. U. 1959, Science, 130, 1421.

Oort, J. H., and Walraven, T. 1956, B.A.N., 12, 285.

Prendergast, K. H. 1964, private communication.

Sandage, A. R. 1961, The Hubble Atlas of Galaxies (Washington: Carnegie Institution of Washington).

Sandage, A. R., and Miller, W. C. 1964, to be published.

Shklovsky, I. S. 1955, Astron. J. U.S.S.R., 32, 215.

Volders, L., and Högbom, J. A. 1961, B.A.N., 15, 307.

Woltjer, L. 1958, B.A.N., 14, 39.

TABLE 1

OBSERVATIONS OF M 82

Spectrum No.	Date	Position Angle	Exposure (Min.)	Position in Galaxy
B 720	Dec. 24, 1960	65°	79	Nucleus centered
B 724	Dec. 27, 1960	83°	55	Nucleus centered
B 725	Dec. 27, 1960	46°	90	Nucleus centered
B 726	Dec. 27, 1960	57°.3	90	Nucleus centered
B 736	Feb. 27, 1961	69°	50	Nucleus centered
B 737	Feb. 28, 1961	69°	150	Nucleus SW end of slit
B 920	Feb. 11, 1962	62°	240	Nucleus SW end of slit*
B 1188	Jan. 10, 1964	145°	85	Crosses major axis 5" SW of nucleus
B 1196	Jan. 14, 1964	0°	90	Nucleus centered
B 1197	Jan. 14, 1964	62°	62	Nucleus centered
B 1198	Jan. 14, 1964	30°	90	Nucleus centered
L 767	Mar. 8, 1964	155°	38	Crosses major axis 10" SW of nucleus

* On this spectrum alone, no emission lines were measured; the absorption lines Hβ, Hγ, Hδ, Hζ, Hη were measured.

TABLE 2

EMISSION LINE

VELOCITIES IN M82 (REDUCED TO LOCAL STANDARD OF REST)

AS A FUNCTION OF DISTANCE FROM ASSUMED CENTER

Distance From Center (Sec. of Arc)	Velocity (km/sec)	Distance From Center (Sec. of Arc)	Velocity (km/sec)	Distance From Center (Sec. of Arc)	Velocity (km/sec)
B 1196	P.A. 0°	B 1196 (Cont.)	P.A. 0°	B 1198	P.A. 30°
Hα:		[N II] 6583:		Hα:	
N -88.2	+383	N -35.5	+284	N.E. -46.3	+413
-85.3	379	-32.5	279	-43.4	363
-82.4	329	-29.7	304	-40.5	381
-79.5	333	-26.8	276	-37.6	406
-76.6	284	-23.9	270	-34.7	371
-73.7	302	-21.0	280	-31.9	365
-70.8	283	-18.1	266	-29.0	338
-67.9	286	-15.2	253	-26.1	355
-65.0	327	-12.3	300	-23.2	380
-62.1	262	- 9.4	301	-20.3	382
-59.2	288	- 6.5	325	-17.4	406
-56.3	291	- 3.6	327	-14.5	393
-53.4	317	- 0.7	298	-11.6	342
-50.6	312	+ 2.2	336	- 8.7	328
-47.6	307	+ 5.1	277	- 5.8	330
-44.7	295	+ 8.0	248	- 2.9	316
-41.8	282	+10.9	211	0	287
-38.9	300	+13.8	204	+ 2.9	288
-36.1	317	+16.6	182	+ 5.8	251
-33.2	327	+19.5	168	+ 8.7	290
-30.3	345	+22.4	168	+11.6	253
-27.4	317	+25.3	160	+14.5	231
-24.5	319	+28.2	198	+17.4	239
-21.6	328	+31.1	198	+20.3	224
-18.7	308	+34.0	213	+23.2	225
-15.8	309	S +36.9	212	+26.1	263
-12.9	251	[S II] 6717:		+29.0	225
-10.0	282	N - 7.8	296	+31.9	240
- 7.1	284	- 4.9	333	+34.8	232
+10.3	215	- 2.0	305	+37.6	232
+13.2	200	+ 0.9	306	+40.5	209
+16.1	201	+ 3.8	307	+43.4	193
+19.0	201	+ 6.7	242	+46.3	185

	+21.9	201		+ 9.6	235		+49.2	169
	+24.8	186		+12.5	221	S.W.	+52.1	198
	+27.7	209		+15.3	214	[N II] 6583:		
	+30.5	216		+18.2	193	N.E.	-19.8	432
	+33.4	209		+21.1	185		-16.9	441
	+36.3	238		+24.0	142		-14.0	420
	+39.2	230	S	+26.9	119		-11.1	399
	+42.1	237	[S II] 6731:				- 8.3	371
	+45.0	214	N	- 6.5	318		- 5.7	342
	+47.9	220		- 3.6	341		- 2.5	329
	+50.8	204		- 0.7	335		+ 0.4	322
	+53.7	173		+ 2.2	343		+ 3.3	293
	+56.6	179		+ 5.1	300		+ 6.2	272
	+59.5	170		+ 8.0	250		+ 9.1	235
	+62.4	146		+10.9	243		+12.0	251
	+65.3	151		+13.8	193		+14.9	236
	+68.2	127		+16.6	186		+17.8	252
	+71.1	125		+19.5	186		+20.7	245
	+74.0	160		+22.4	157		+23.6	230
	+76.9	105	S	+25.4	178		+26.5	238
	+79.8	110					+29.4	223
S	+82.6	93					+32.3	260

TABLE 2 (Continued)

Distance From Center (Sec. of Arc)	Velocity (km/sec)
B 1198 (Cont.)	P.A. 30°
[N II] 6583:	
+35.2	+237
+38.1	274
+41.0	274
+43.9	258
+46.8	250
+49.7	257
+52.6	218
+55.5	187
+58.3	170
S.W. +61.2	184
[S II] 6717:	
N.E. - 4.8	315
- 1.9	287
+ 1.0	303
+ 3.9	303
+ 6.8	261
+ 9.7	218
+12.6	160
+15.5	153
+18.4	154
S.W. +21.3	190
[S II] 6731:	
N.E. - 4.9	341
- 2.0	350
+ 0.9	351
+ 3.8	366
+ 6.7	330
+ 9.6	259
+12.5	187
S.W. +15.3	152
B 725	P.A. 46°
Hα:	
N.E. -10.0	318

Distance From Center (Sec. of Arc)	Velocity (km/sec)
B 725 (Cont.)	P.A. 46°
[N II] 6583:	
+ 2.9	+254
+ 5.8	270
+ 8.7	241
+11.6	257
+14.5	212
+17.4	228
+20.3	213
+23.2	206
+26.1	214
+29.0	214
+31.9	206
+34.8	206
S.W. +37.7	168
[S II] 6717:	
N.E. - 6.6	329
- 3.7	294
- 0.8	207
+ 2.1	179
+ 5.0	157
+ 7.9	180
+10.8	144
+13.7	166
+16.6	159
+19.5	166
+22.4	196
+25.3	173
S.W. +28.2	202
[S II] 6731:	
N.E. - 6.6	363
- 3.7	386
- 0.8	387
+ 2.1	359
+ 5.0	316
+ 7.9	302

Distance From Center (Sec. of Arc)	Velocity (km/sec)
B 726 (Cont.)	P.A. 57°.3
Hα:	
+16.6	+216
+19.5	197
+22.4	179
+25.3	175
+28.2	157
+31.1	161
+34.0	165
+36.9	146
+39.8	127
+42.7	139
+45.6	128
+48.5	139
+51.4	181
S.W. +54.3	162
[N II] 6583:	
N.E. -36.6	404
-33.7	357
-30.8	356
-27.9	331
-15.8	398
-12.9	350
-10.0	348
- 7.1	368
- 4.2	358
- 1.3	355
+ 1.6	330
+ 4.5	342
+ 7.4	324
+10.3	291
+13.2	257
+16.1	246
+19.0	243
+21.8	202
+24.7	222

where T is the age of the explosion. The philosophy behind this approach is that it attempts above all to minimize the energy requirements by ignoring the possible presence of a proton flux, and by supposing that the electrons which were produced in a single outburst are still able to radiate the observed fluxes of optical and radio radiation. Since

$$t_{\frac{1}{2}} = \frac{8.35 \times 10^{-3}}{H_{\perp}^{2} E} \text{ years}$$

where E is measured in Bev and

$$\nu_c = 1.61 \times 10^{13} H_{\perp} E^2 \text{ c/s},$$

this means that, for the optical synchrotron radiation, ($\nu_c \approx 6 \times 10^{14}$ c/s) $E = 5.4 \times 10^{12}$ ev and $H_{\perp} = 1.2 \times 10^{-6}$ gauss. Then the total energies in particles and field are

$$E_R = 2.6 \times 10^{56} \text{ ergs}$$

and

$$E_M = 1.3 \times 10^{52} \text{ ergs}.$$

Thus the bulk of the energy of the explosion has been released in the form of kinetic energy of gas and ultra-relativistic electrons (even the lowest-energy electrons responsible for radio radiation at 100 Mc have energies of $\sim$5 Bev). A negligible fraction is contained in magnetic field energy. In the other two optical synchrotron sources which are known, the Crab Nebula (Oort and Walraven 1956, Woltjer 1958, Burbidge 1958) and the jet in M 87 (Shklovsky 1955, Burbidge 1956) rather different conditions are thought to prevail. In the Crab a number of arguments have led to the conlusion that the magnetic field has a strength somewhere in the range 5×10^{-4} - 10^{-2} gauss so that the half-lives of the range 40,000 - 50 years are involved. In each of these cases it is clear that the time scales for the decay of the optical electrons are much shorter than the time scales associated with the explosive phenomena as they can be

TABLE 2 (Continued)

Distance From Center (Sec. of Arc)	Velocity (km/sec)
B 726 (Cont.)	P.A. 57°.3
[S II] 6717:	
+24.2	+166
+27.1	148
+30.0	122
+32.9	185
+35.7	144
+38.6	111
+41.5	122
S.W. +44.4	74
[S II] 6731:	
N.E. - 5.4	343
- 2.5	341
+ 0.4	338
+ 3.3	350
+ 6.2	293
+ 9.1	300
+12.0	275
+14.9	221
+17.8	232
+20.7	244
+23.6	233
+26.5	200
+29.4	219
+32.3	208
+35.2	189
+38.0	208
+41.0	204
S.W. +43.9	229
B 1197	P.A. 62°
Hα:	
N.E. -37.3	420
-34.4	398
-31.5	406
-28.6	368

Distance From Center (Sec. of Arc)	Velocity (km/sec)
B 1197 (Cont.)	P.A. 62°
Hα:	
S.W. +63.3	+153
[N II] 6583:	
N.E. -30.8	320
-27.9	335
-25.0	327
-22.1	320
-19.2	320
-16.3	327
-13.4	334
-10.5	310
- 7.6	332
- 4.7	339
- 1.8	315
+ 1.1	276
+ 3.9	275
+ 6.8	236
+ 9.7	212
+12.6	196
+15.5	186
+18.4	169
+21.3	167
+24.2	173
+27.1	156
+30.0	161
+32.9	174
+35.8	164
+38.7	154
+41.6	166
+44.5	156
+47.4	138
+50.3	143
+53.2	177
+56.1	144
S.W. +59.0	149

Distance From Center (Sec. of Arc)	Velocity (km/sec)
B 1197 (Cont.)	P.A. 62°
[S II] 6731:	
+26.8	+183
+29.7	160
S.W. +32.6	172
B 720	P.A. 65°.5
Hα:	
N.E. -43.2	359
-40.3	329
-37.4	353
-34.5	383
-31.6	383
-28.7	414
-25.8	376
-22.9	398
-20.0	390
-17.1	428
-14.3	420
-11.4	404
- 8.5	411
- 5.6	372
- 2.7	363
+ 0.2	324
+ 3.1	307
+ 6.0	291
+ 8.9	266
+11.8	242
+14.7	270
+17.6	246
+20.5	251
+23.4	234
+26.3	240
+29.2	245
+32.1	227
+35.0	255

-25.7	353	[S II] 6717:		+37.9	223
-22.8	315	N.E. - 2.1	305	S.W. +40.8	250
-19.9	330	+ 0.8	260	[N II] 6583:	
-17.0	322	+ 3.7	252	N.E. -44.2	340
-14.1	329	+ 6.6	236	-41.3	356
-11.3	291	+ 9.4	191	-38.4	349
- 8.4	305	+12.3	161	-35.5	342
- 5.5	304	+15.2	123	-32.7	350
+10.3	184	+18.1	114	-29.7	387
+19.9	117	S.W. +21.1	149	-26.8	380
+22.8	123	[S II] 6731:		-24.0	418
+25.7	113	N.E. - 2.1	314	-21.1	447
+28.6	126	+ 0.8	284	-18.2	432
+31.5	131	+ 3.7	254	-15.3	446
+34.4	152	+ 6.6	260	-12.4	453
+37.2	142	+ 9.4	230	- 9.5	430
+40.1	154	+12.3	156	- 6.6	421
+43.0	174	+15.2	147	- 3.7	390
+45.9	171	+18.1	138	- 0.8	351
+51.7	165	+21.0	165	+ 2.1	335
+57.5	129	+23.9	164	+ 5.0	326

TABLE 2 (Continued)

Distance From Center (Sec. of Arc)	Velocity (km/sec)	Distance From Center (Sec. of Arc)	Velocity (km/sec)	Distance From Center (Sec. of Arc)	Velocity (km/sec)
B 720 (Cont.)	P.A. 65°.5	B 736 (Cont.)	P.A. 69°	B 736 (Cont.)	P.A. 69°
[N II] 6583:		Hα:		[S II] 6731:	
+ 7.9	+264	-13.6	+464	- 1.8	+314
+10.8	277	-10.7	431	+ 1.1	289
+13.7	253	- 7.8	383	+ 4.0	286
+16.6	258	- 4.9	380	+ 6.9	269
+19.5	264	- 2.0	354	+ 9.8	251
+22.4	262	+ 0.9	306	+12.6	248
+25.3	207	+ 3.8	280	+15.5	208
+28.2	220	+ 6.8	247	S.W. +18.4	169
+31.1	172	+ 9.7	206		
+34.0	140	+12.5	188	B 737	P.A. 69°
+36.9	145	+15.4	207	Hα:	
+39.7	157	+18.3	219	N.E. -35.1	399
+42.6	185	+21.2	193	-32.2	380
+45.5	243	+24.1	205	-29.4	391
S.W. +48.4	202	+27.0	156	-26.5	425
[S II] 6717:		+30.0	145	-23.6	391
N.E. -15.1	418	S.W. +32.8	157	-20.7	402
-12.2	381	[N II] 6583:		-17.8	391
- 9.3	388	N.E. -29.0	342	-14.9	364
- 6.4	351	-26.2	363	-12.0	345
- 3.5	357	-23.3	406	- 9.1	356
- 0.6	320	-20.4	381	- 6.1	322
+ 2.3	304	-17.5	394	- 3.3	288
+ 5.1	289	-14.6	362	- 0.4	291
+ 8.0	287	-11.7	382	S.W. + 2.5	234
+10.9	242	- 8.8	387	[N II] 6583:	
+13.8	255	- 5.9	332	N.E. -35.1	400
+16.7	247	- 3.0	314	-32.2	396
+19.6	216	- 0.1	288	-29.4	415
+22.5	185	+ 2.8	240	-26.5	426
+25.4	219	+ 5.7	230	-23.6	423
+28.3	159	+ 8.6	227	-20.7	419
+31.2	164	+11.5	201	-17.8	400
+34.1	154	+14.4	175	-14.9	396

S.W. +37.0	166		+17.3	187	-12.0	400
[S II] 6731:			+20.2	192	- 9.1	358
N.E. -14.0	455		+23.1	211	- 6.2	377
-11.1	418		+26.0	162	- 3.3	403
- 8.2	447	S.W.	+28.9	144	- 0.4	369
- 5.3	403	[S II] 6717:			S.W. + 2.5	312
- 2.4	395	N.E.	-16.3	488	[S II] 6717:	
+ 0.5	343		-13.4	493	N.E. -36.9	439
+ 3.4	342		-10.5	395	-34.0	428
+ 6.3	319		- 7.6	378	-31.1	475
+ 9.2	288		- 4.7	346	-28.2	493
+12.0	294		- 1.8	292	-25.4	496
+15.0	293		+ 1.1	245	-22.4	412
S.W. +17.9	262		+ 4.0	242	-19.5	415
			+ 6.8	203	-16.6	396
B 736	P.A. 69°	S.W.	+ 9.7	156	-13.7	377
Hα:		[S II] 6731:			-10.8	373
N.E. -25.1	434	N.E.	-13.4	382	- 7.9	303
-22.2	417		-10.5	372	- 5.0	291
-19.3	423		- 7.6	348	- 2.1	279
-16.5	458		- 4.7	316	S.W. + 0.8	209

TABLE 2 (Continued)

Distance From Center (Sec. of Arc)	Velocity (km/sec)
B 737 (Cont.)	P.A. 69°
[S II] 6731:	
N.E. -37.5	+458
-34.6	512
-31.7	530
-28.8	475
-25.9	442
-23.0	467
-20.1	398
-17.2	422
-14.3	389
-11.4	363
- 8.5	351
- 5.6	304
- 2.7	292
+ 0.2	259
S.W. + 3.1	225

Distance From Center (Sec. of Arc)	Velocity (km/sec)
B 724 (Cont.)	P.A. 83°
[S II] 6717:	
N.E. - 6.6	+372
- 3.7	337
- 0.8	354
+ 2.1	334
+ 5.0	262
+ 7.9	263
+10.8	191
S.W. +13.7	178
[S II] 6731:	
N.E. - 3.6	390
- 0.7	377
+ 2.2	320
+ 5.1	292
+ 8.0	250
+10.9	244
S.W. +13.8	201

Distance From Center (Sec. of Arc)	Velocity (km/sec)
B 724	P.A. 83°
Hα:	
N.E. -32.8	369
-29.9	357
-27.0	375
-24.2	393
-21.2	380
-18.3	321
-15.4	354
-12.5	364
- 9.6	366
- 6.8	383
- 3.9	369
- 1.0	340
+ 1.9	311
+ 4.8	290
+ 7.7	268
+10.6	246

Distance From Major Axis (Sec. of Arc)	Velocity (km/sec)
B 1188 (Cont.)	P.A. 145°
	+11.7	+211
	+14.6	247
	+17.5	275
	+20.4	251
	+23.3	272
	+26.2	270
	+29.1	231
	+32.0	213
	+34.9	226
	+37.8	217
	+40.7	237
	+43.6	264
	+46.5	254
	+49.4	312
	+52.3	279
	+55.2	306
	+58.1	326
	+61.0	300
	+63.8	290
	+66.7	347
	+69.6	344
N.W. +72.5	363
[N II] 6583:	
S.E. -43.9	102
-41.0	125
-38.1	141
-35.3	142
-32.4	187
-29.5	188
-26.6	173
-23.7	188
-20.8	196
-17.9	203
-15.0	218

Distance From Major Axis (Sec. of Arc)	Velocity (km/sec)
B 1188 (not through nucleus)	P.A. 145°
Hα:	
S.E. -86.7	131
-83.8	126
-80.9	167
-78.0	117
-75.1	112
-72.2	145
-69.3	155
-66.5	217
-63.6	182
-60.7	138
-57.8	185
-54.9	210
-52.0	226

+13.5	216	-49.1	220	-12.1	218
+16.4	179	-46.2	229	- 9.2	232
+19.3	179	-43.3	237	- 6.3	232
+22.2	225	-40.4	223	- 3.4	231
+25.1	233	-37.5	194	- 0.5	230
+28.0	226	-34.6	187	+ 2.4	244
+30.9	211	-31.7	195	+ 5.3	229
S.W. +33.8	188	-28.8	196	+ 8.2	235
[N II] 6583:		-25.9	219	+11.1	219
N.E. - 5.2	382	-23.0	234	+14.0	210
- 2.3	376	-20.1	211	+16.9	238
+ 0.6	324	-17.2	196	+19.8	199
+ 3.5	303	-14.3	211	+22.7	190
+ 6.4	281	-11.4	218	+25.6	173
+ 9.3	236	- 8.5	225	+28.4	179
+12.2	222	- 5.6	224	+31.3	170
+15.1	200	- 2.8	209	+34.2	212
+18.0	185	+ 0.1	238	+37.1	210
+20.9	247	+ 3.0	229	+40.0	253
+23.8	277	+ 5.9	243	+42.9	243
S.W. +26.7	255	+ 8.8	220	+45.8	278

TABLE 2 (Continued)

Distance From Major Axis (Sec. of Arc)	Velocity (km/sec)
B 1188 (Cont.) P.A. 145°	
[N II] 6583:	
+48.7	+282
+51.6	295
N.W. +54.5	337
[S II] 6717:	
S.E. -15.1	197
-12.2	233
- 9.3	241
- 6.4	248
- 3.5	283
- 0.6	247
+ 2.3	224
+ 5.2	274
+ 8.1	259
N.W. +11.0	279
[S II] 6731:	
S.E. -14.0	220
-11.1	199
- 8.3	213
- 5.4	242
- 2.5	248
+ 0.4	262
+ 3.3	269
+ 6.2	225
N.W. + 9.1	238
L 767 P.A. 155° (not through nucleus)	
[N II] 6548:	
N.W. - 3.7	186
- 2.0	182
- 0.3	164

Distance From Major Axis (Sec. of Arc)	Velocity (km/sec)
L 767 P.A. 155°	
[N II] 6548:	
+ 1.3	+177
+ 3.0	190
+ 4.7	181
+ 6.4	172
S.E. + 8.1	176
Hα:	
N.W. -11.3	148
- 9.6	166
- 8.0	179
- 6.3	170
- 4.6	188
- 2.9	183
- 1.3	205
+ 0.4	196
+ 2.1	192
+ 3.8	178
+ 5.5	169
+ 7.1	178
+ 8.8	169
+10.5	147
+12.2	138
+13.8	124
+15.5	119
+17.2	128
+18.9	128
S.E. +20.6	132
[N II] 6583:	
N.W. -11.2	154
- 9.5	145
- 7.8	154

Distance From Major Axis (Sec. of Arc)	Velocity (km/sec)
L 767 (Cont.) P.A. 155°	
[N II] 6583:	
- 6.1	+149
- 4.4	154
- 2.8	171
- 1.1	198
+ 0.6	193
+ 2.3	184
+ 3.9	188
+ 5.6	171
+ 7.3	175
+ 9.0	161
S.E. +10.7	161
[S II] 6717:	
N.W. - 7.9	172
- 6.2	172
- 4.5	185
- 2.9	171
- 1.2	163
+ 0.5	158
+ 2.2	150
+ 3.9	162
S.E. + 5.5	154
[S II] 6731:	
N.W. - 8.6	169
- 6.9	164
- 5.2	173
- 3.5	177
- 1.8	182
- 0.2	199
+ 1.5	177
+ 3.2	181
S.E. + 4.9	177

TABLE 3

MEAN ABSORPTION LINE VELOCITIES FROM SPECTRUM B 920

Distance From Center (Sec. of Arc)	Velocity and Mean Error* (km/sec)	Distance From Center (Sec. of Arc)	Velocity and Mean Error* (km/sec)
N.E. -146	298 ± 71	-67	308 ± 34
-133	327 ±100	-59	224 ± 29
-125	451 ±106	-52	287 ± 40
-117	406 ± 88	-45	296 ± 55
-110	434 ± 66	-38	199 ± 81
-103	437 ± 57	-31	128 ±105
- 96	426 ± 65	-23	193 ± 67
- 88	384 ± 44	-16	155 ± 67
- 81	386 ± 46	- 7.8	175 ± 49
- 74	370 ± 39	S.W. + 1.9	118 ± 31

*At each position, the velocity is a mean of 5 measures; one each from Hβ, Hγ, Hδ, Hζ, Hη.

FIGURE CAPTIONS

Fig. 1 M 82, photographed at prime focus of McDonald 82-inch telescope on Eastman Kodak 103a-O plate (20-minute exposure). Solid lines mark slit orientations and regions over which emission line velocities were measured (lines drawn black or white simply for best visibility against background). Short broken lines indicate positions where only continuum radiation was observed. The long dashed line in P.A. 62° marks the region over which absorption line velocities were measured. Scale: 1 mm = 2".0.

Fig. 2 A 1-minute exposure of M 82, photographed at prime focus of 82-inch telescope, on Eastman Kodak 103a-O plate, showing details of structure near center. Scale: 1 mm = 2".73. North is at left, east at top.

Fig. 3a Spectrum of M 82 from λ 3600 - λ 6750, photographed at prime focus of McDonald 82-inch telescope on 103a-F emulsion. Left: B1197, P.A. 62°; right: B1198, P.A. 30°. Key for spectral features: 1 = [S II] λ 6731, λ 6716; 2 = [N II] λ 6583, Hα, [N II] λ 6548; 3 = NaI λ 5893 absorption and He I λ 5876 emission; 4 = [O II] λ 5007; 5 = Hβ; 6 = Hγ; 7 = [O II] λ 3727. Velocity variations are shown by [S II], Hα, and [N II] lines. Wavelengths of some lines in comparison spectrum are shown.

Fig. 3b Red spectral region of M 82, showing velocity variations in emission lines of [S II], [N II], and Hα. a: B720, P.A. 65½°; b: B724, P.A. 83°; c: B1188, P.A. 145°; d: B1196, P.A. 0°.

Fig. 4 Measured velocities in M 82 along major axis, reduced to local standard of rest, plotted against distance from assumed center. Solid line is adopted rotation curve from Mayall's absorption line measures.

Fig. 5 Measured emission line velocities in P.A. 0°, reduced to local standard of rest, plotted against distance from assumed center.

Fig. 6 Measured emission line velocities in P.A. 30°, reduced to local standard of rest, plotted against distance from assumed center.

Fig. 7 Measured emission line velocities in P.A. 65°.5 reduced to local standard of rest, plotted against distance from assumed center.

Fig. 8 Measured emission line velocities in P.A. 69°, reduced to local standard of rest, plotted against distance from assumed center.

Fig. 9 Measured emission line velocities in P.A. 83°, reduced to local standard of rest, plotted against distance from assumed center.

Fig. 10 Measured emission line velocities in P.A. 145°, B 1188, reduced to local standard of rest, plotted against distance from where slit crosses major axis. Velocities in P.A. 142° (≡ 322°) and P.A. 155° (≡ 335°) from Lynds and Sandage are shown, although their measures refer to positions displaced along major axis (by about 10") from spectrum B 1188.

Fig. 11 Measured emission line velocities in P.A. 155°, Lick spectrum L 767, reduced to local standard of rest, plotted against distance from where slit crosses major axis.

Fig. 12 Smoothed emission line vlocities, with respect to center of galaxy, as a function of distance from the center (solid curve) for P.A. = 0°. Adopted rotation curve projected to this position angle is nearly constant (dashed curve), for thin-disk model. Projected rotation curve for thick-disk model is almost indistinguishable from this.

Fig. 13 Smoothed emission line velocities, with respect to center of galaxy, as a function of distance from major axis (solid curve) for P.A. 145°. Adopted rotation curve, projected to this position angle and crossing major axis 5" southwest of nucleus is shown (short-dashed curve), for thin-disk model. Projected rotation curve for thick-disk model is also plotted (long-dashed curve).

Fig. 14 Smoothed emission line velocities, with respect to center of galaxy, as a function of distance from center (solid curve) for P.A. 30°. Note departures from adopted rotation curve projected to P.A. 30° (dashed curve).

Fig. 15 Smoothed emission line velocities, with respect to center of galaxy, as a function of distance from center (solid curve) for P.A. 46°. Note departures from adopted rotation curve projected to P.A. 46° (dashed curve).

Fig. 16 Smoothed emission line velocities, with respect to center of galaxy, as a function of distance from center (solid curve) for P.A. 57°.3. Note departures from adopted rotation curve projected to P.A. 57°.3 (dashed curve).

Fig. 17 Smoothed emission line velocities, with respect to center of galaxy, as a function of distance from center (solid curve) for P.A. 62°. Note departures from adopted rotation curve projected to P.A. 62° (dashed curve).

Fig. 18 Smoothed emission line velocities, with respect to center of galaxy, as a function of distance from center (solid curve) for P.A. 65°.5. Note departures from adopted rotation curve projected to P.A. 65°.5 (dashed curve).

Fig. 19 Smoothed emission line velocities, with respect to center of galaxy, as a function of distance from center (solid curve) for P.A. 69°. Note departures from adopted rotation curve projected to P.A. 69° (dashed curve).

Fig. 20 Smoothed emission line velocities, with respect to center of galaxy, as a function of distance from center (solid curve) for P.A. 83°. Note departures from adopted rotation curve projected to P.A. 83° (dashed curve).

Fig. 21 Sketch of geometry of explosion cone in M 82.

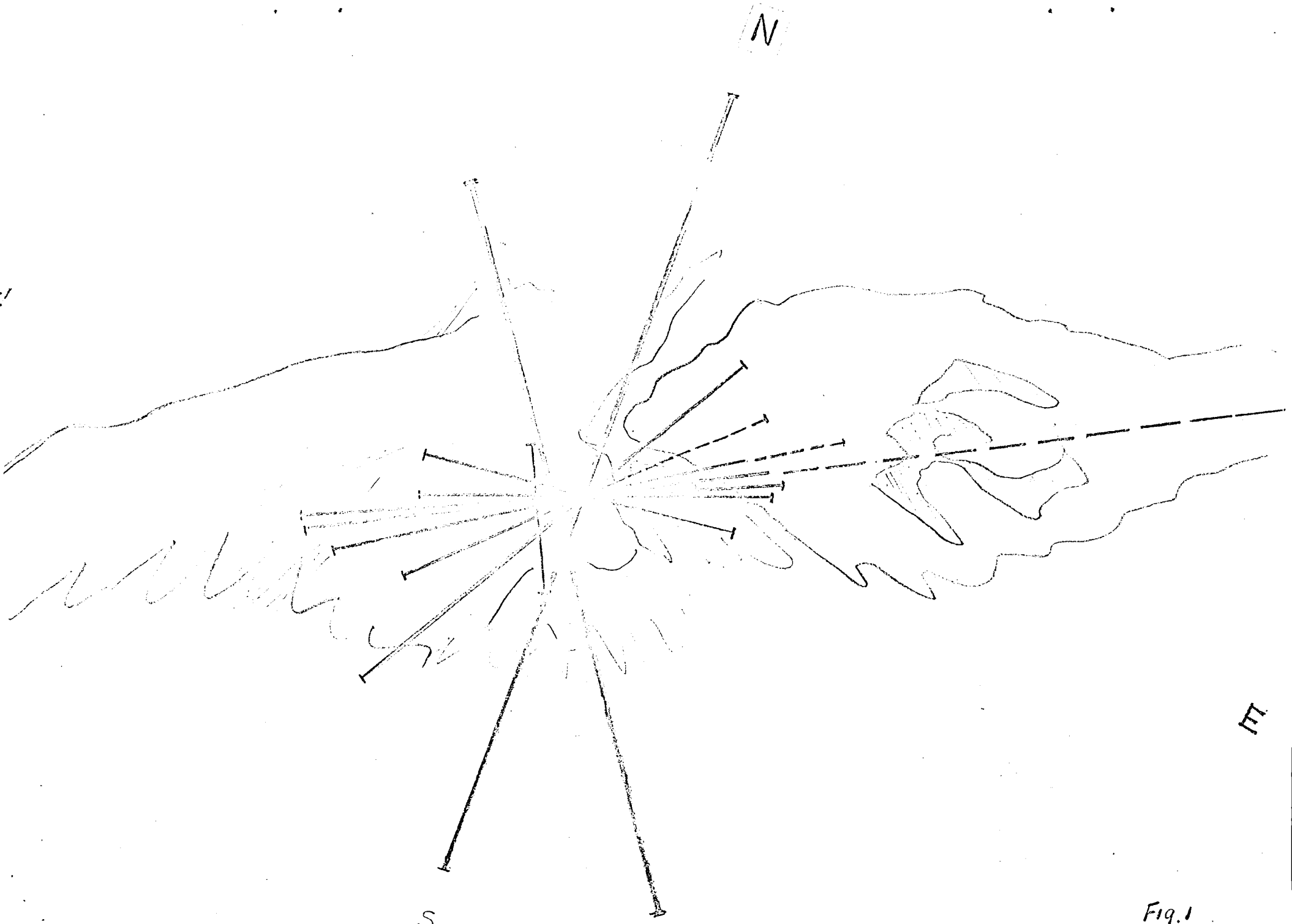

Fig. 1

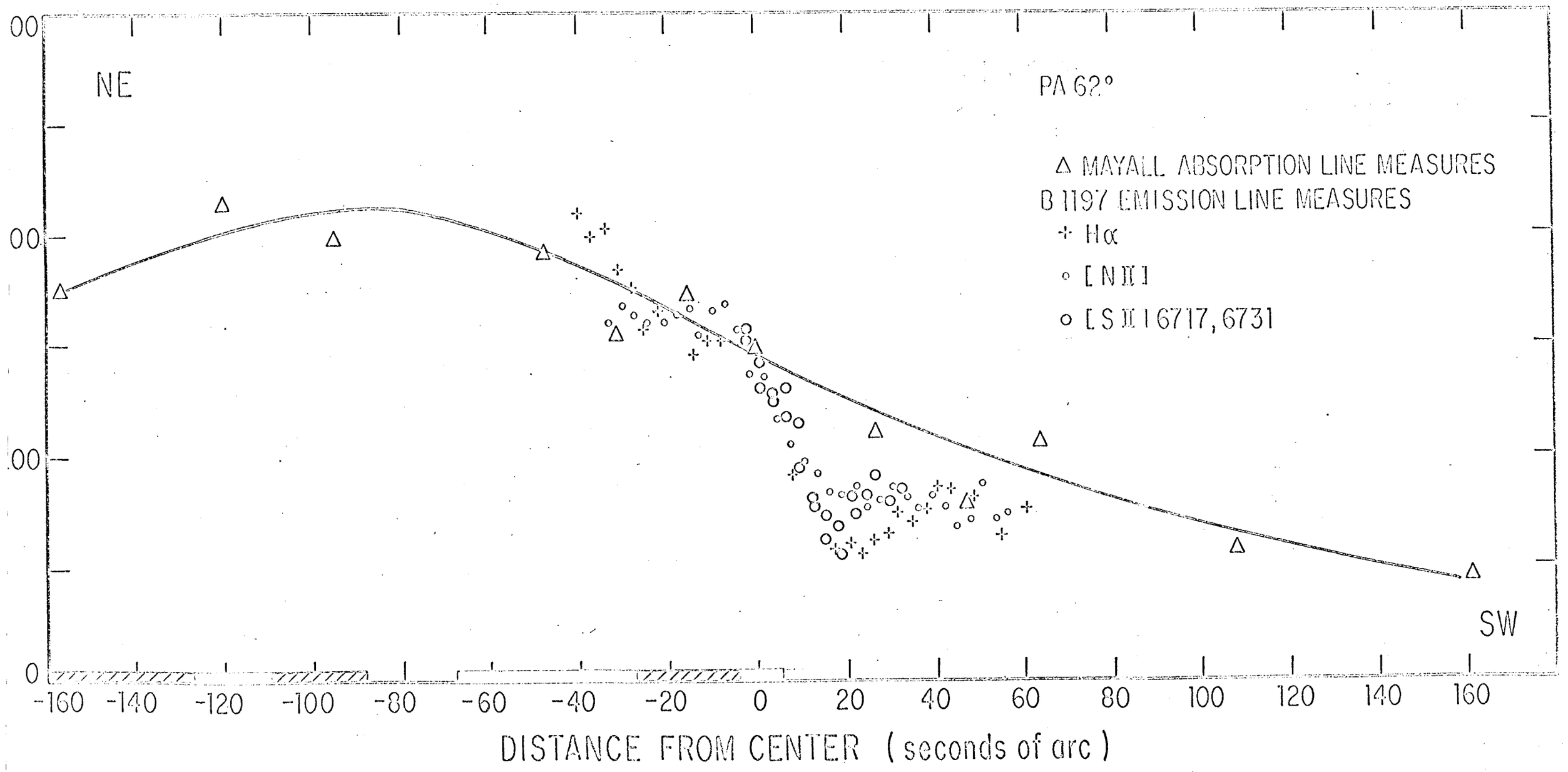
VELOCITY REDUCED TO LOCAL STANDARD OF REST
00
00
00
0
NE
SW
PA 62°
Δ MAYALL ABSORPTION LINE MEASURES
B 1197 EMISSION LINE MEASURES
+ Hα
○ [N II]
○ [S II] 6717, 6731
-160 -140 -120 -100 -80 -60 -40 -20 0 20 40 60 80 100 120 140 160
DISTANCE FROM CENTER (seconds of arc)

Fig. 4

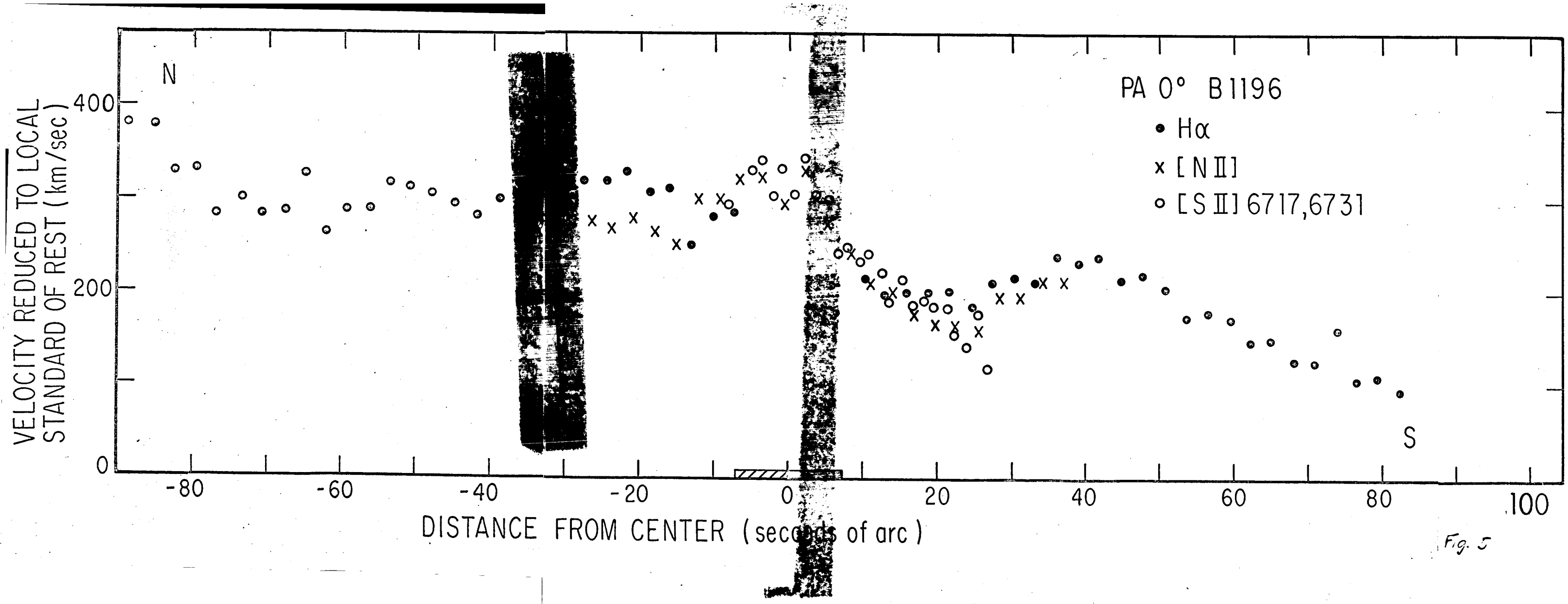
N
S
PA 0° B1196
Hα
[N II]
[S II] 6717,6731
VELOCITY REDUCED TO LOCAL STANDARD OF REST (km/sec)
400
200
0
-80
-60
-40
-20
0
20
40
60
80
100
DISTANCE FROM CENTER (seconds of arc)

Fig. 5

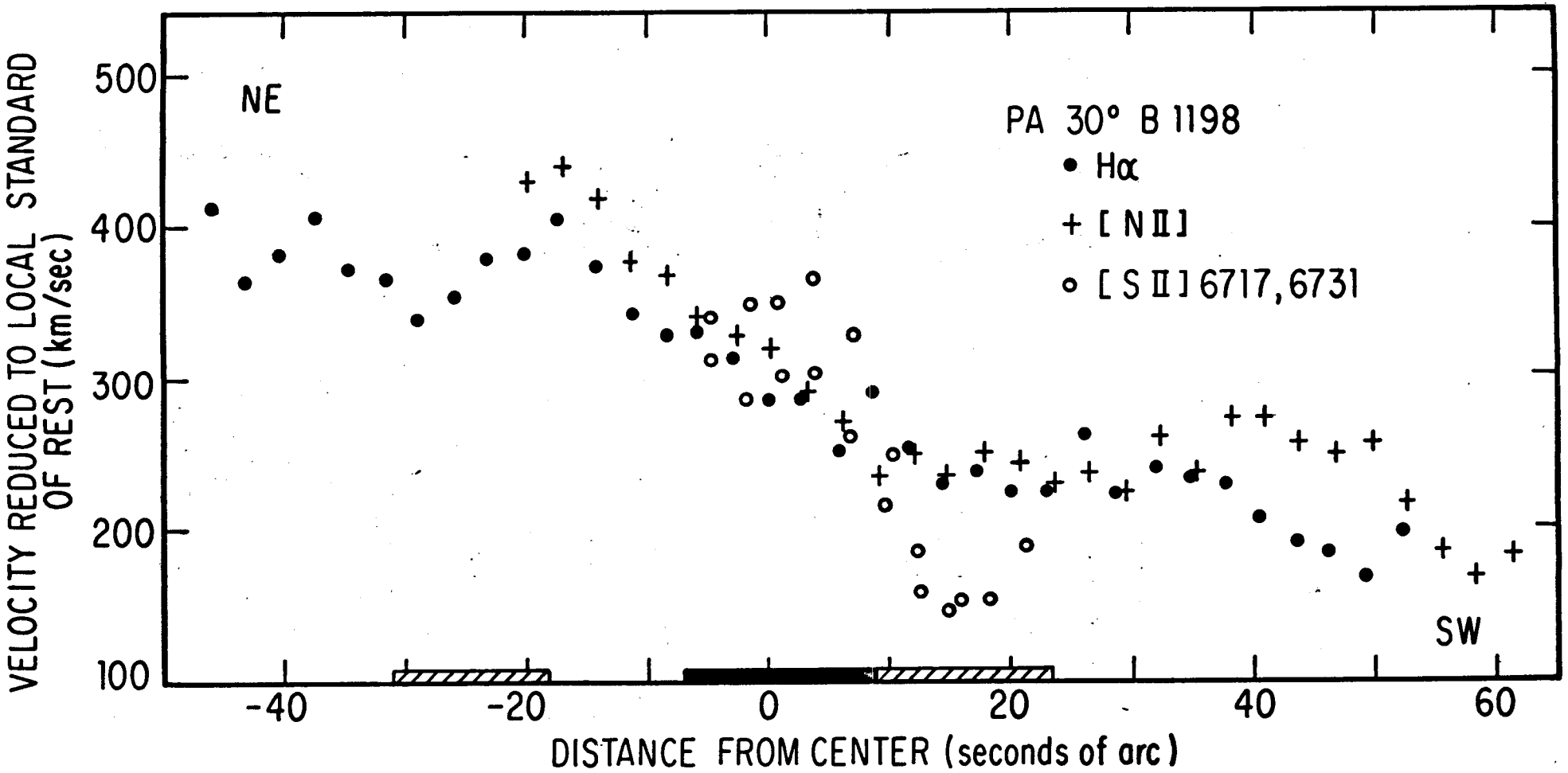
NE
SW
PA 30° B 1198
• Hα
+ [N II]
○ [S II] 6717, 6731
VELOCITY REDUCED TO LOCAL STANDARD OF REST (km/sec)
500
400
300
200
100
-40
-20
0
20
40
60
DISTANCE FROM CENTER (seconds of arc)

Fig. 6

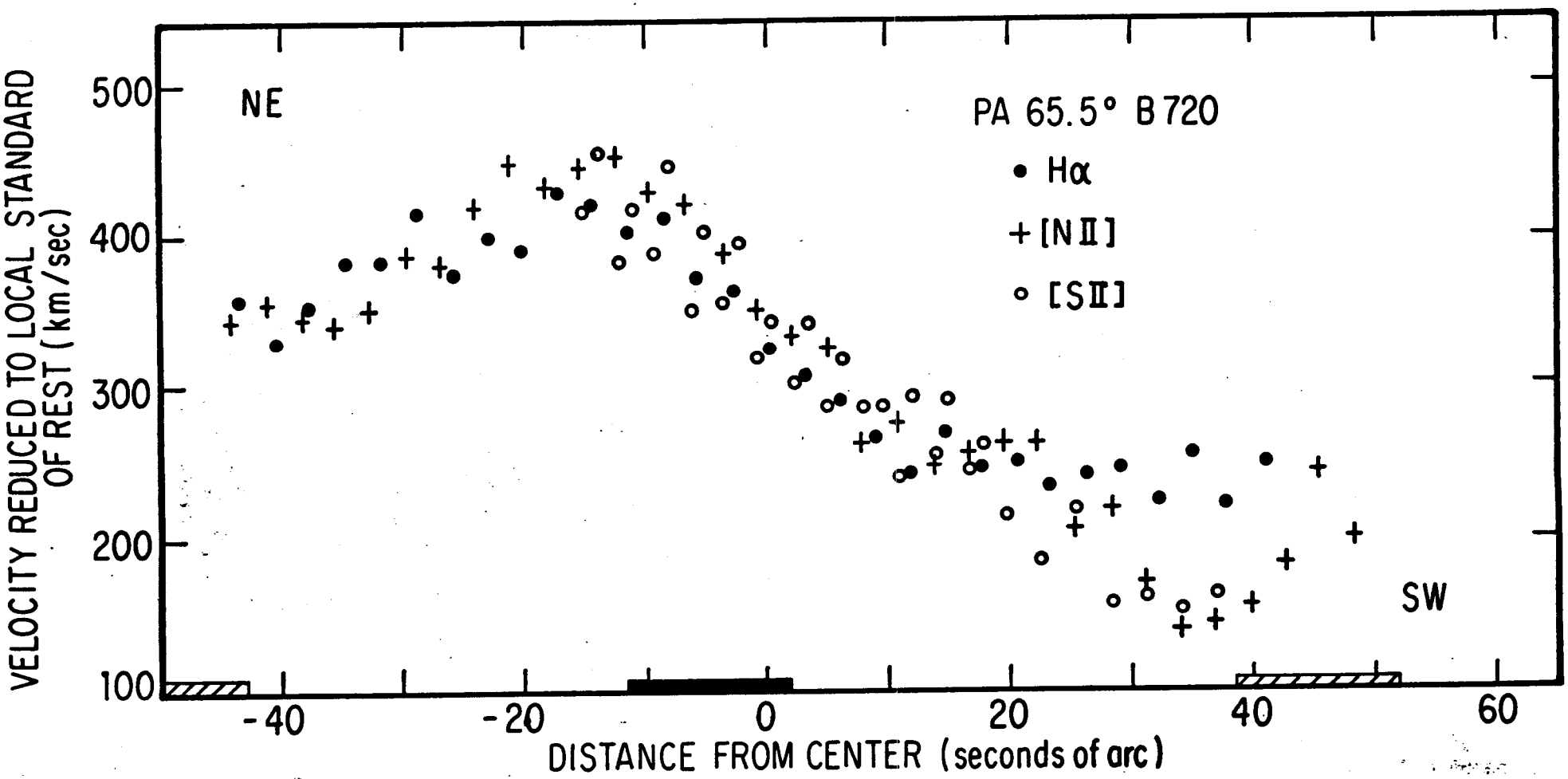
NE
PA 65.5° B720
• Hα
+ [NII]
○ [SII]
SW
VELOCITY REDUCED TO LOCAL STANDARD OF REST (km/sec)
500
400
300
200
100
-40
-20
0
20
40
60
DISTANCE FROM CENTER (seconds of arc)

Fig. 7

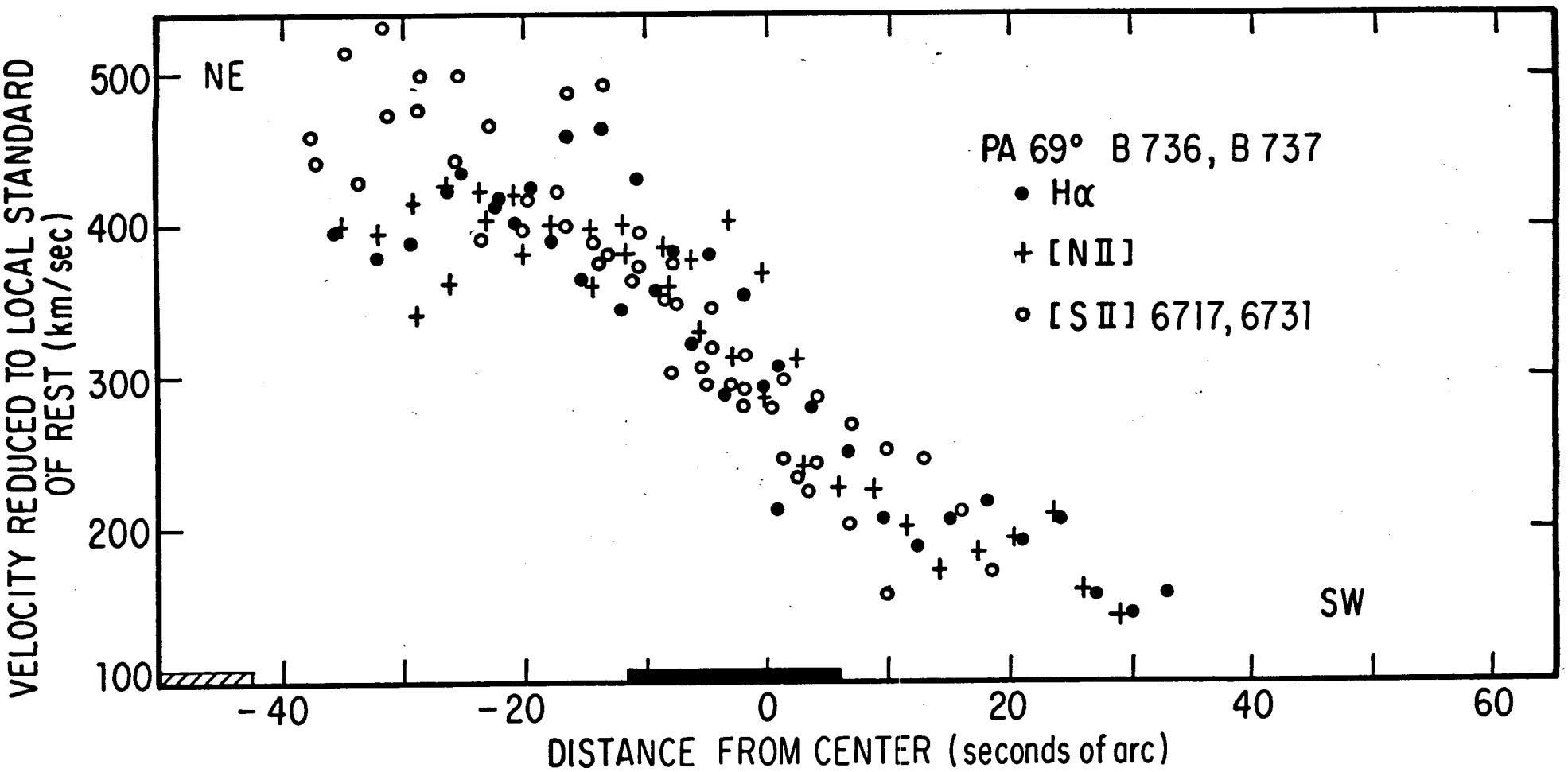
VELOCITY REDUCED TO LOCAL STANDARD OF REST (km/sec)
500
400
300
200
100
NE
SW
PA 69° B 736, B 737
• Hα
+ [N II]
○ [S II] 6717, 6731
-40
-20
0
20
40
60
DISTANCE FROM CENTER (seconds of arc)

Fig. 8

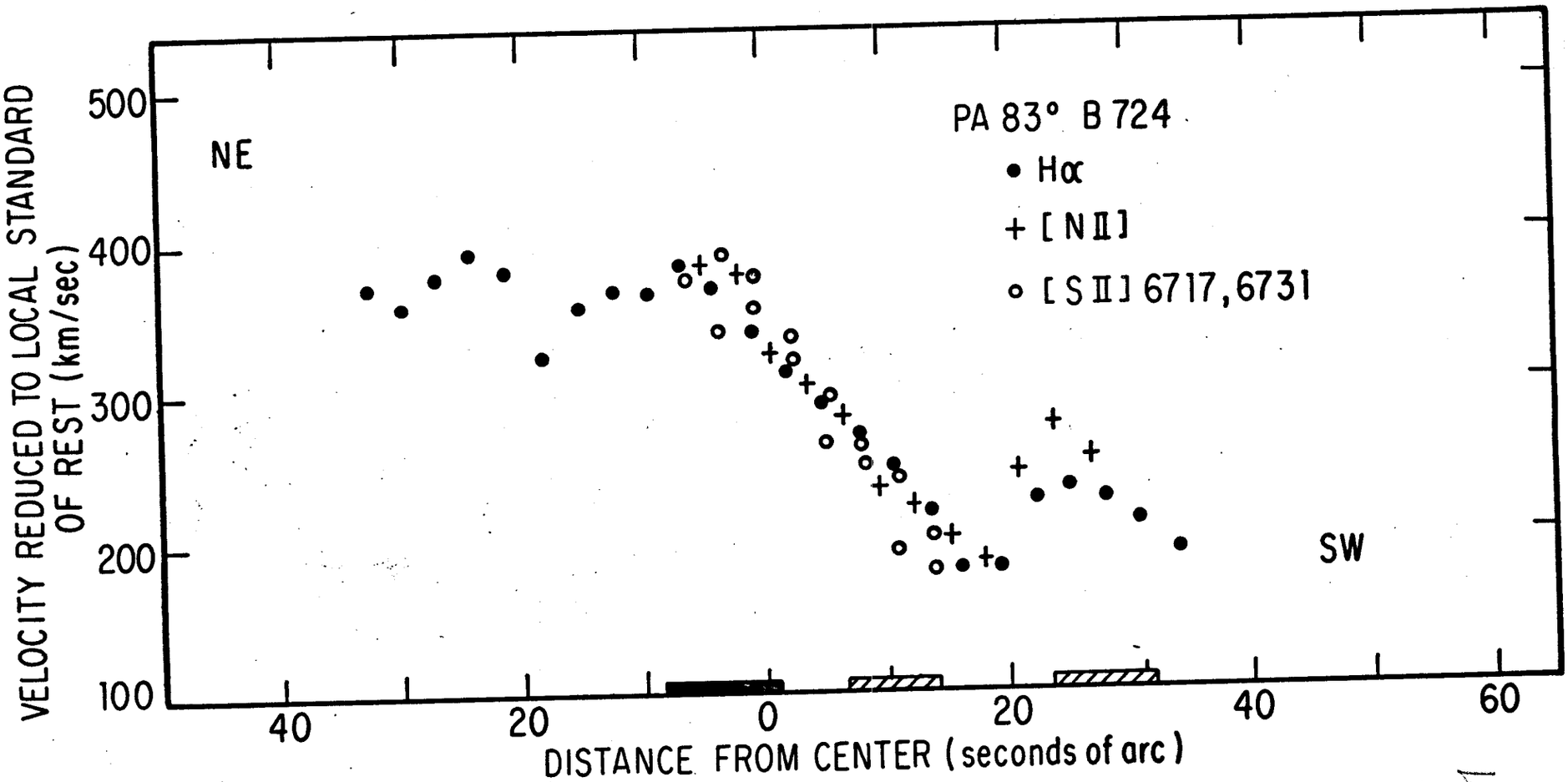
VELOCITY REDUCED TO LOCAL STANDARD OF REST (km/sec)
500
400
300
200
100
NE
SW
PA 83° B 724
• Hα
+ [N II]
○ [S II] 6717, 6731
40
20
0
20
40
60
DISTANCE FROM CENTER (seconds of arc)

Fig. 9

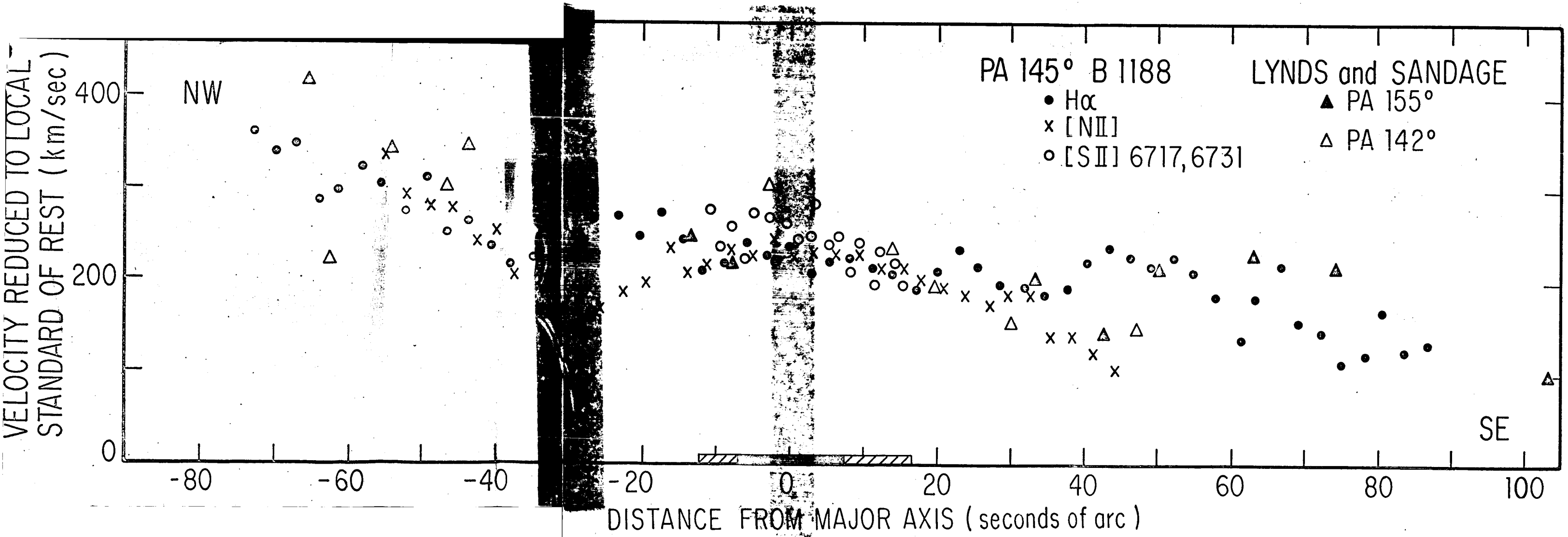
PA 145° B 1188
LYNDS and SANDAGE
• Hα
× [NII]
○ [SII] 6717,6731
▲ PA 155°
△ PA 142°
NW
SE
VELOCITY REDUCED TO LOCAL STANDARD OF REST (km/sec)
400
200
0
-80
-60
-40
-20
0
20
40
60
80
100
DISTANCE FROM MAJOR AXIS (seconds of arc)

Fig. 10

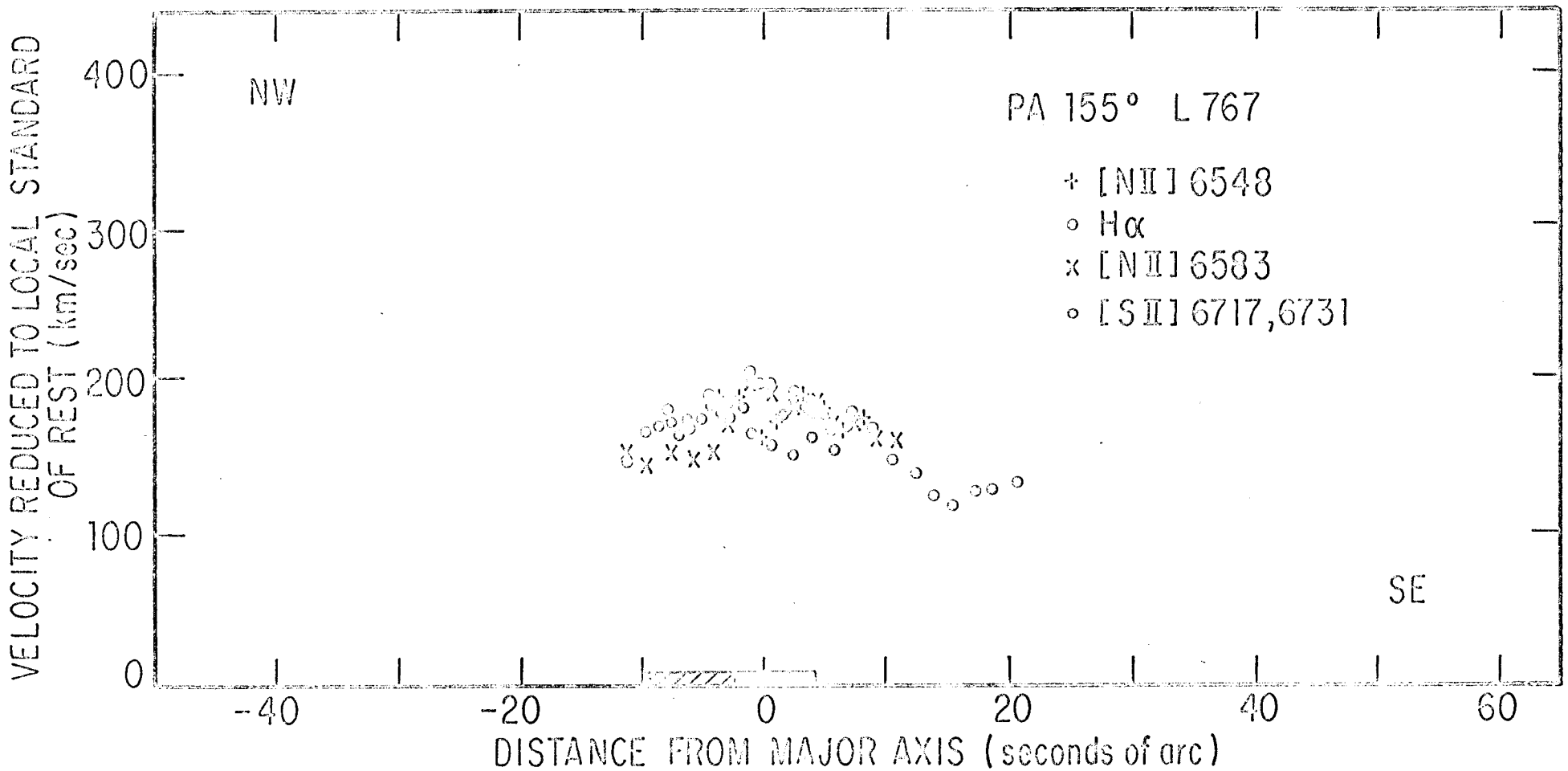
NW
SE
PA 155° L 767
+ [NII] 6548
∘ Hα
× [NII] 6583
∘ [SII] 6717,6731
VELOCITY REDUCED TO LOCAL STANDARD OF REST (km/sec)
400
300
200
100
0
-40
-20
0
20
40
60
DISTANCE FROM MAJOR AXIS (seconds of arc)

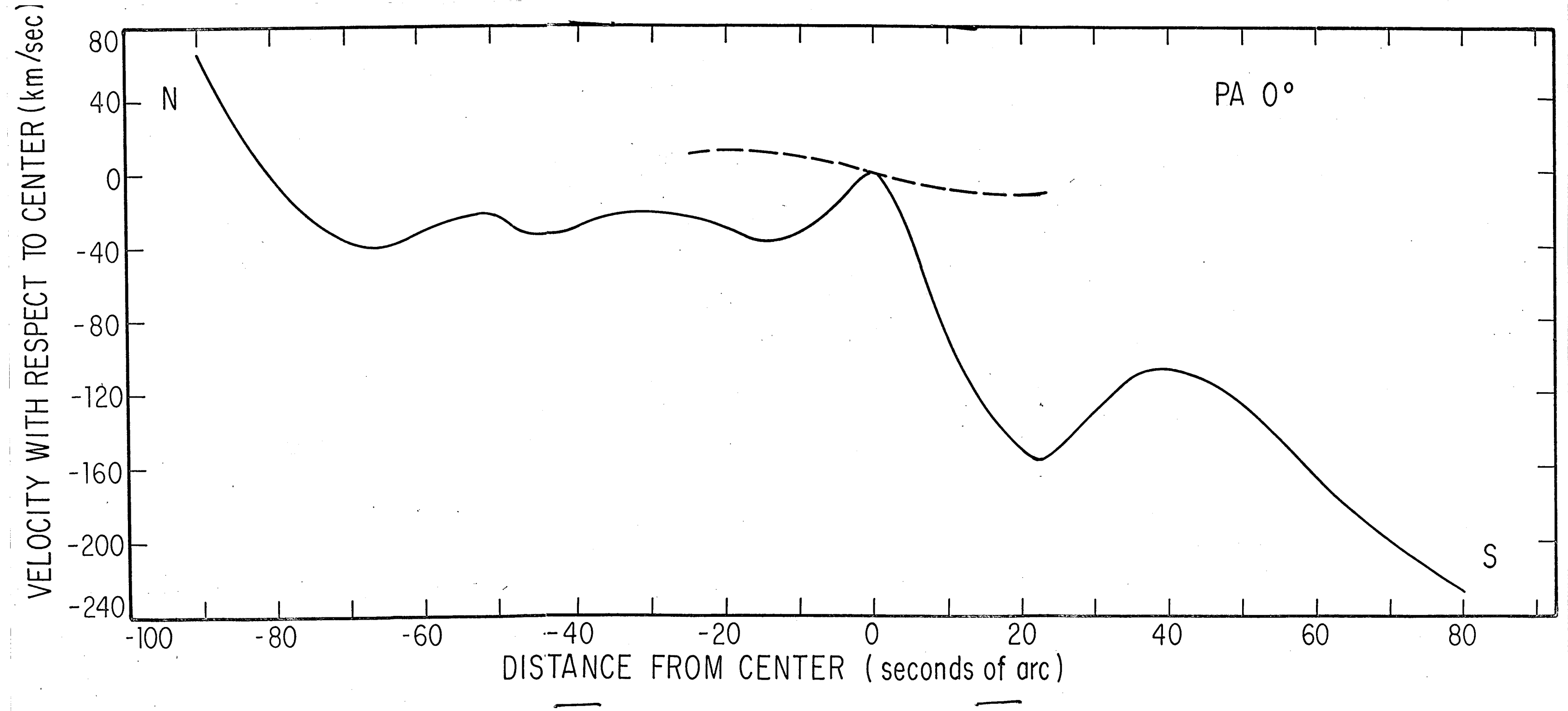
VELOCITY WITH RESPECT TO CENTER (km/sec)
80
40
0
-40
-80
-120
-160
-200
-240
N
S
PA 0°
-100
-80
-60
-40
-20
0
20
40
60
80
DISTANCE FROM CENTER (seconds of arc)

Fig. 2

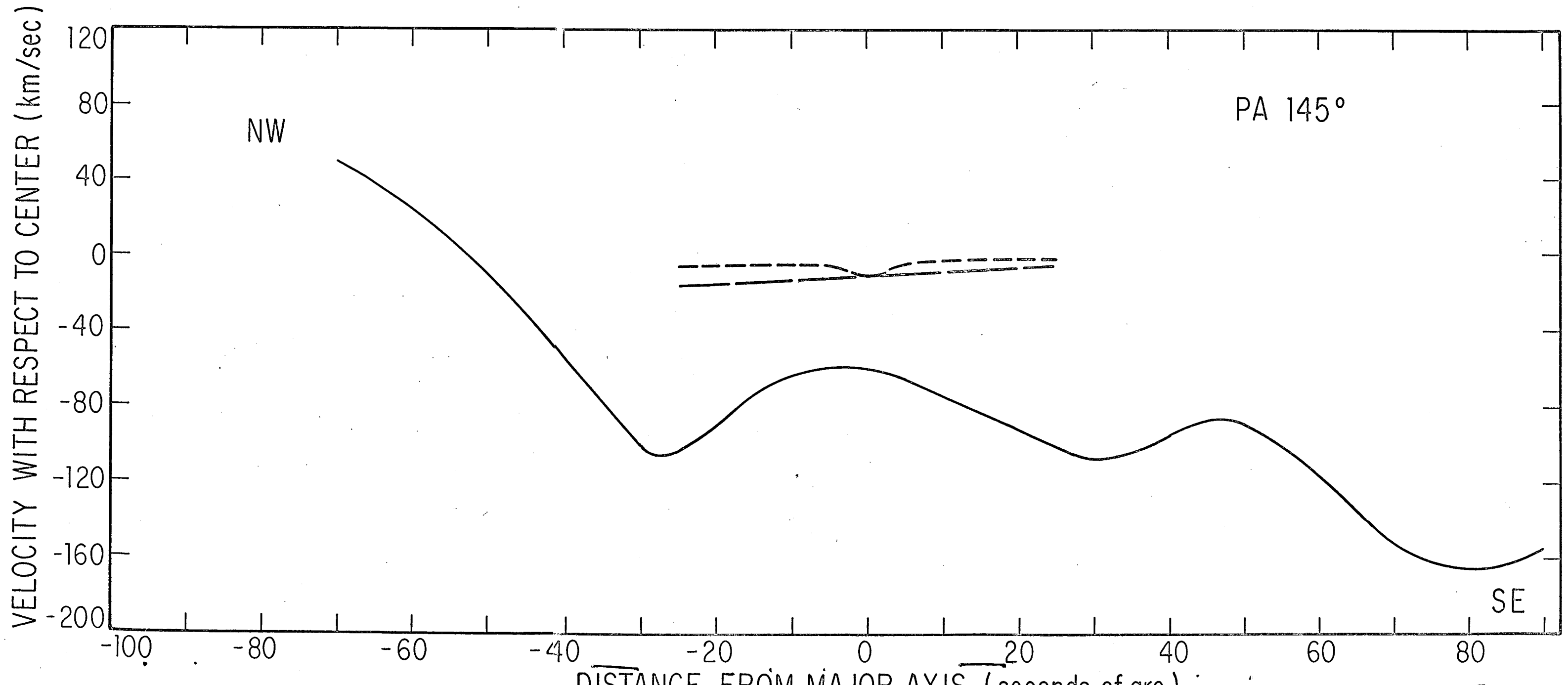
VELOCITY WITH RESPECT TO CENTER (km/sec)
120
80
40
0
-40
-80
-120
-160
-200
NW
PA 145°
SE
-100
-80
-60
-40
-20
0
20
40
60
80
DISTANCE FROM MAJOR AXIS (seconds of arc)

Fig. 13

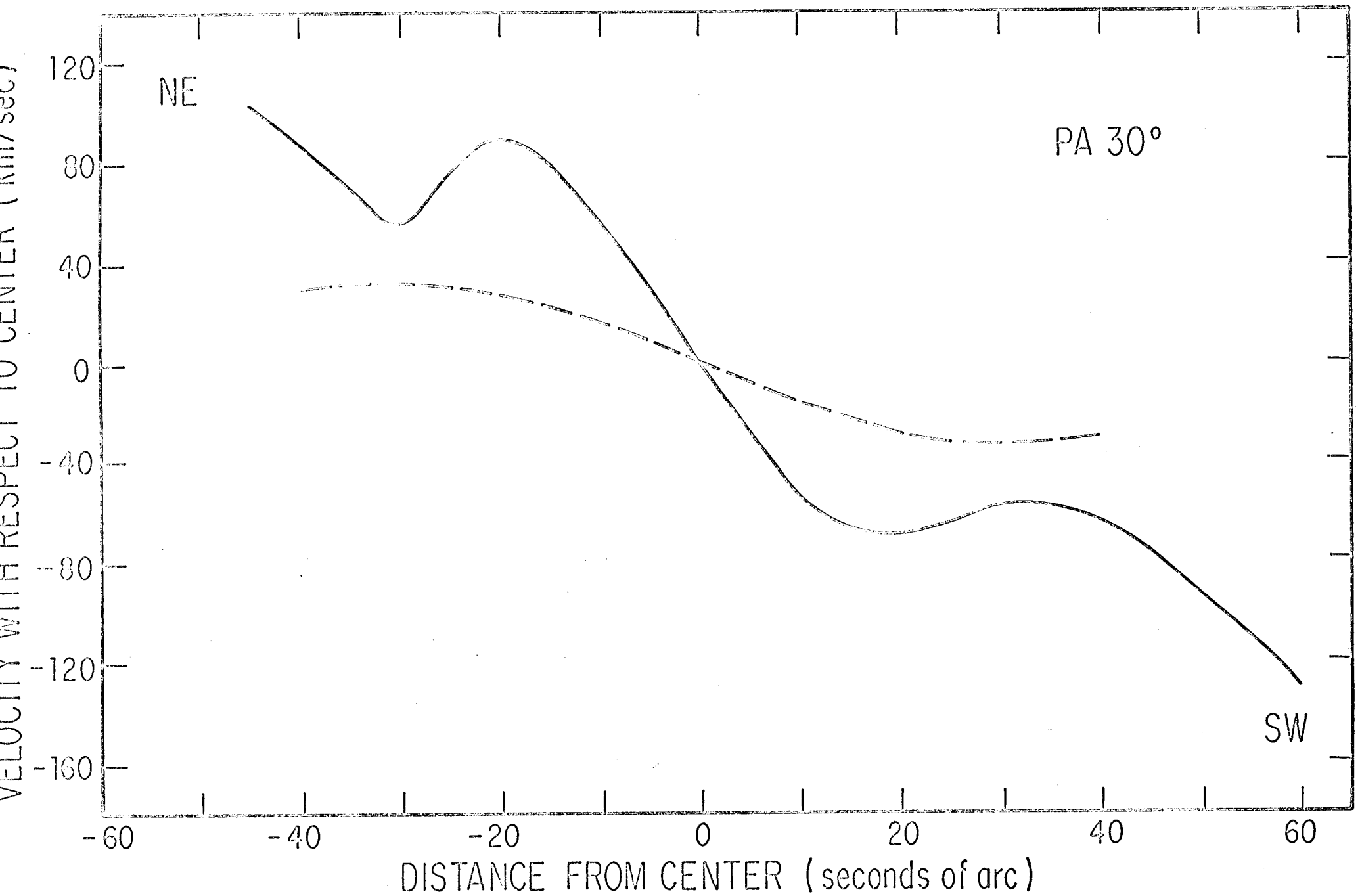
NE
PA 30°
SW
120
80
40
0
-40
-80
-120
-160
-60
-40
-20
0
20
40
60
VELOCITY WITH RESPECT TO CENTER (KM/SEC)
DISTANCE FROM CENTER (seconds of arc)

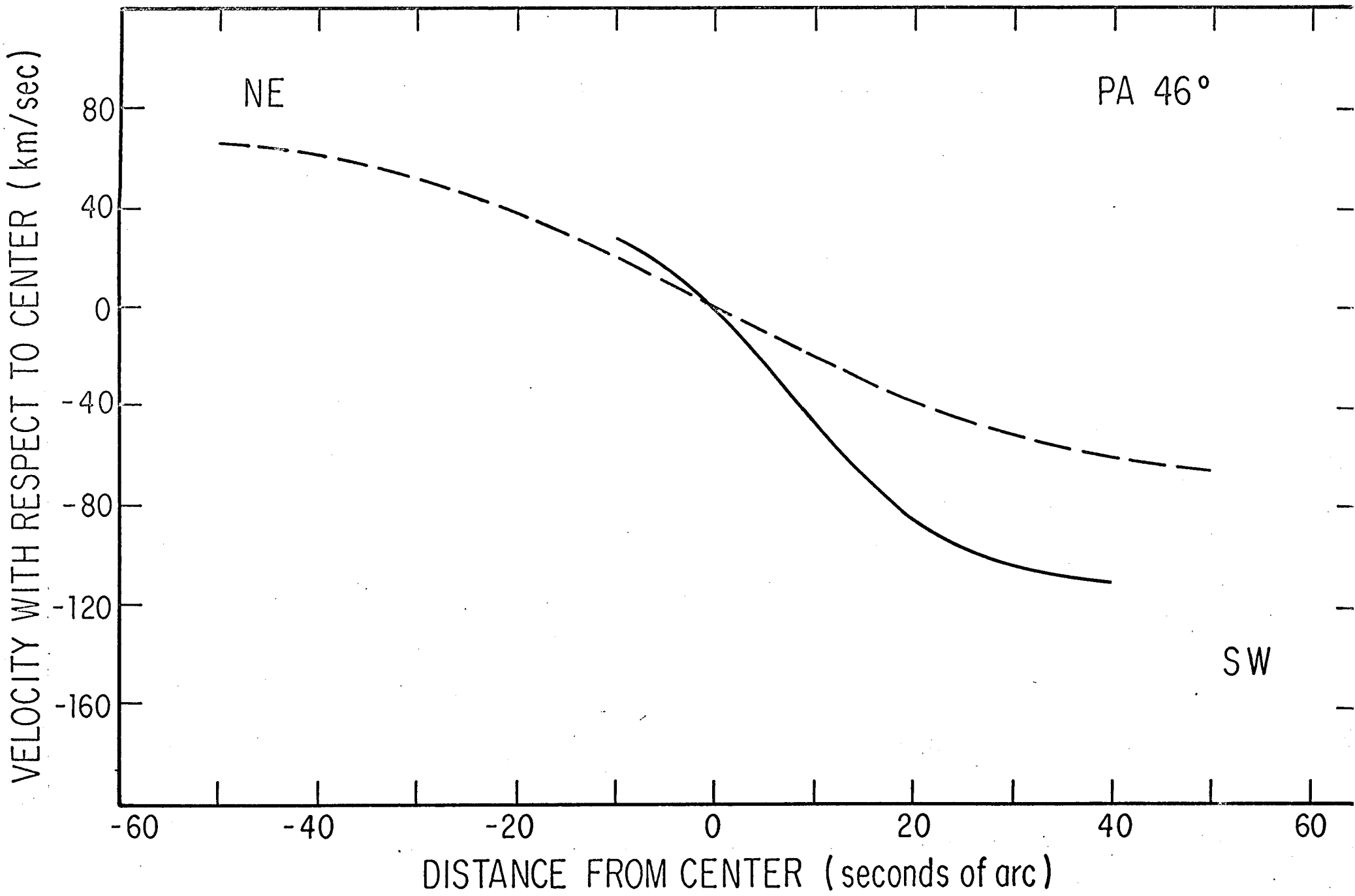
NE
PA 46°
SW
VELOCITY WITH RESPECT TO CENTER (km/sec)
80
40
0
-40
-80
-120
-160
-60
-40
-20
0
20
40
60
DISTANCE FROM CENTER (seconds of arc)

Fig. 15

15

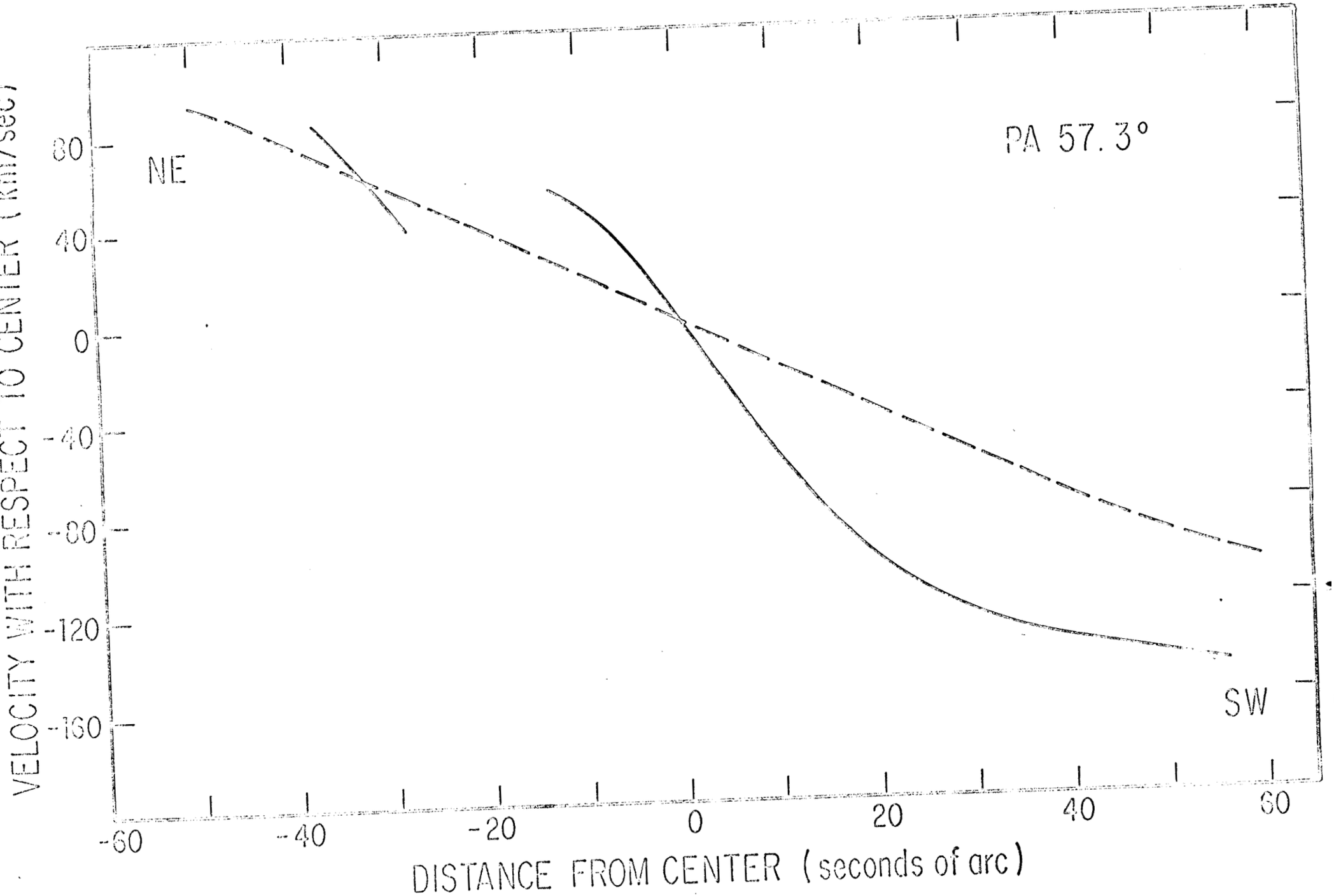
PA 57.3°
NE
SW
80
40
0
-40
-80
-120
-160
VELOCITY WITH RESPECT TO CENTER (km/sec)
-60
-40
-20
0
20
40
60
DISTANCE FROM CENTER (seconds of arc)

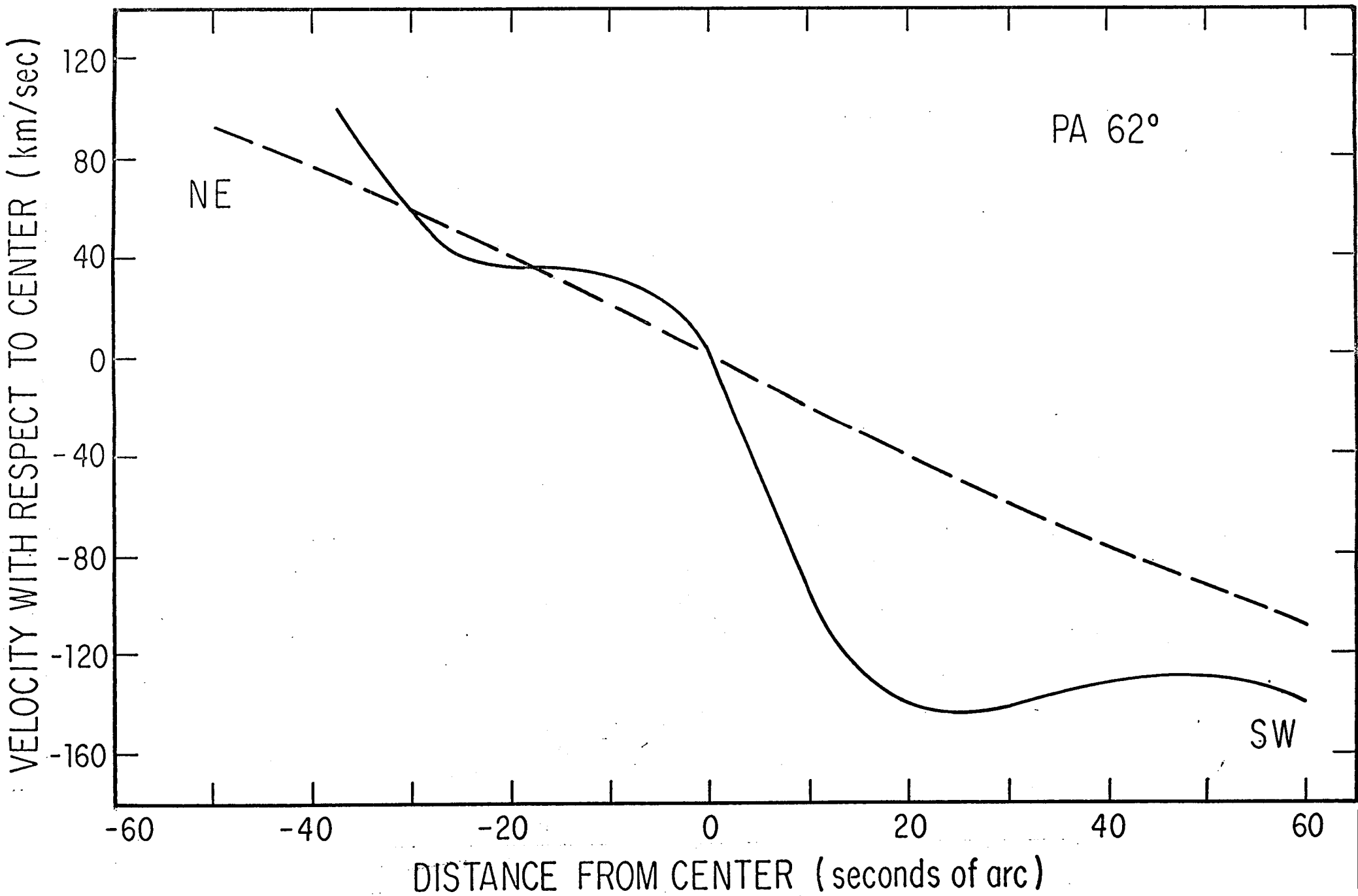
VELOCITY WITH RESPECT TO CENTER (km/sec)
120
80
40
0
-40
-80
-120
-160
PA 62°
NE
SW
-60
-40
-20
0
20
40
60
DISTANCE FROM CENTER (seconds of arc)

Fig. 1

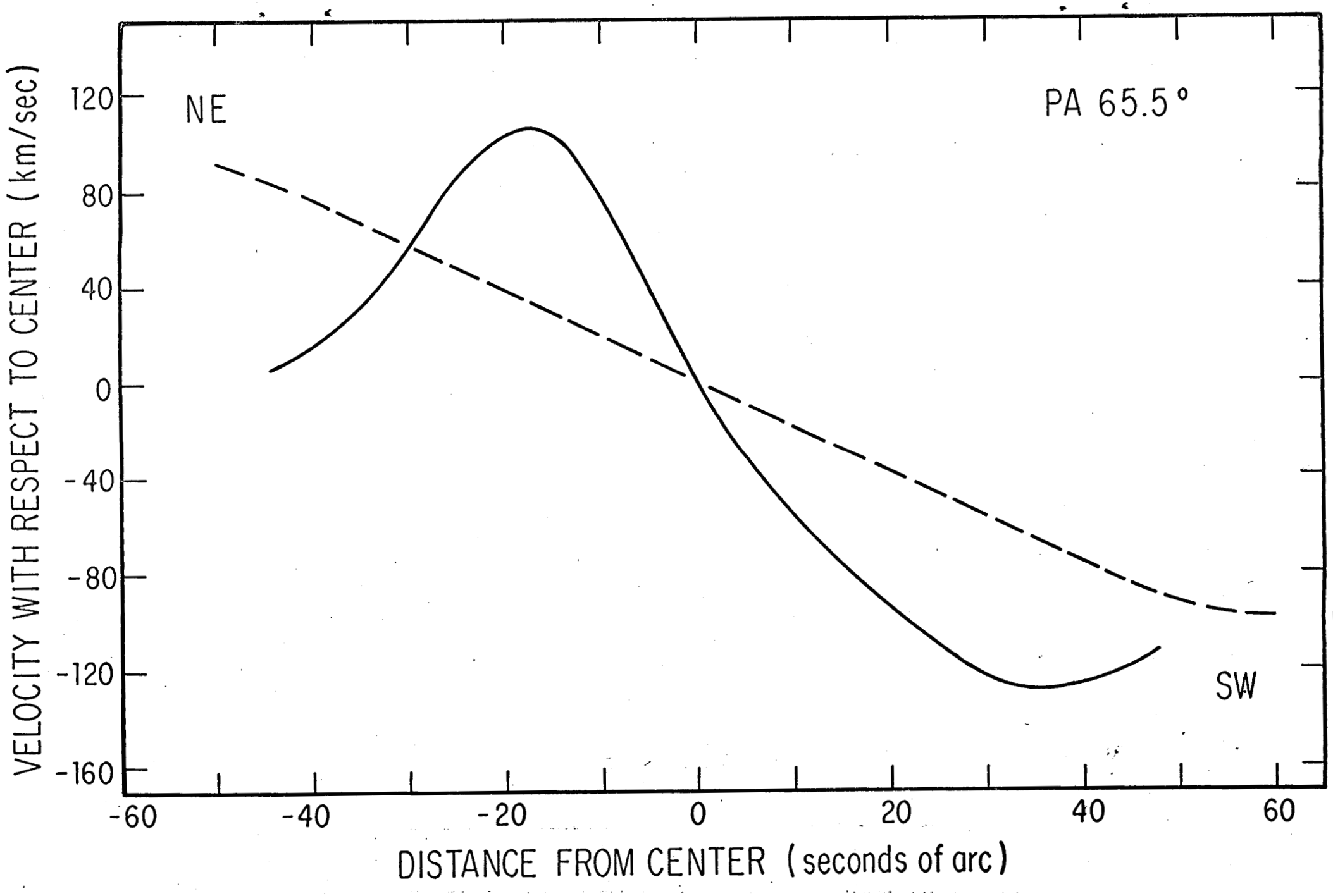
NE
PA 65.5°
SW
120
80
40
0
-40
-80
-120
-160
-60
-40
-20
0
20
40
60
VELOCITY WITH RESPECT TO CENTER (km/sec)
DISTANCE FROM CENTER (seconds of arc)

Fig. 18

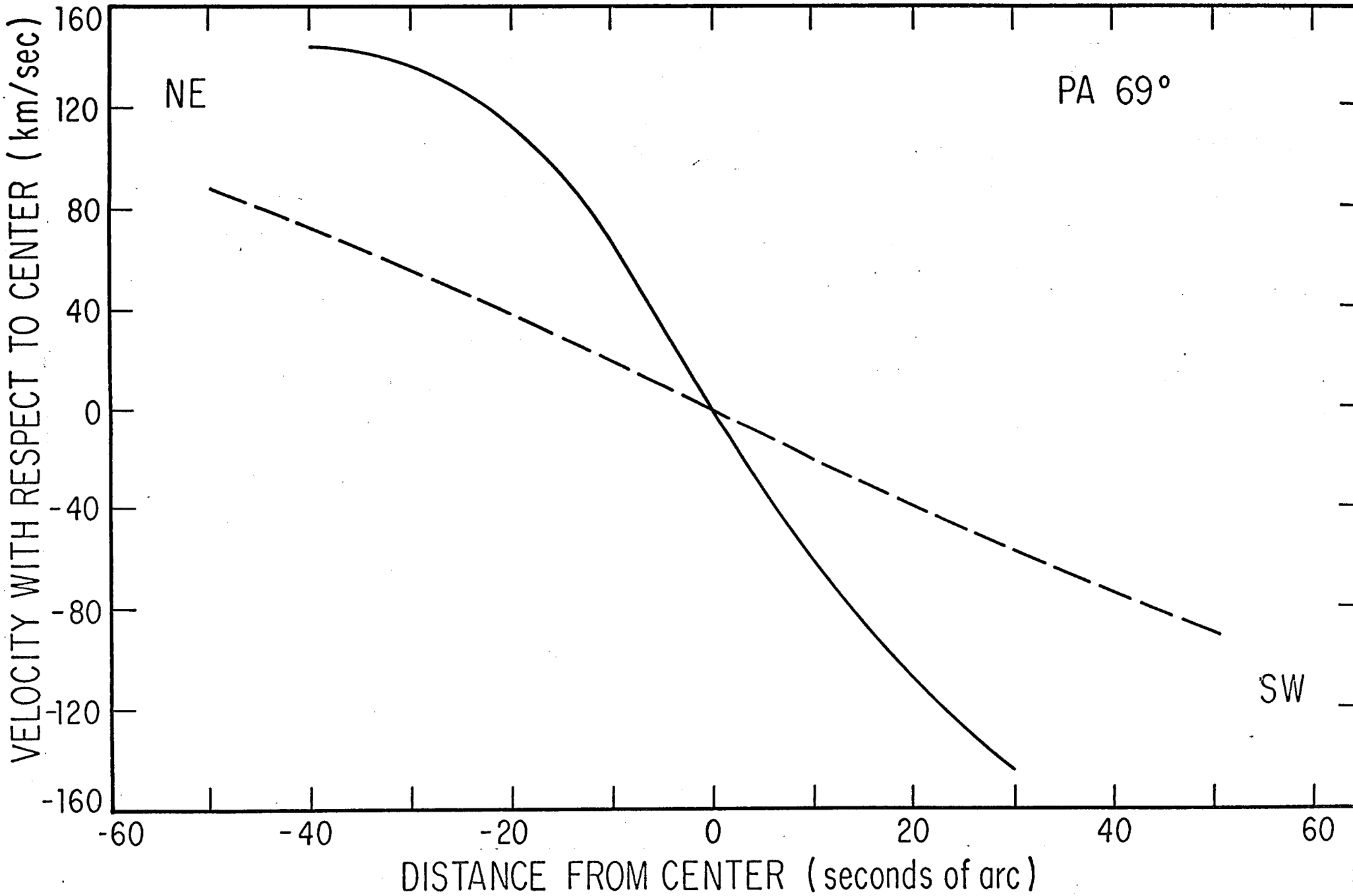
NE
PA 69°
SW
VELOCITY WITH RESPECT TO CENTER (km/sec)
160
120
80
40
0
-40
-80
-120
-160
-60
-40
-20
0
20
40
60
DISTANCE FROM CENTER (seconds of arc)

Fig. 11

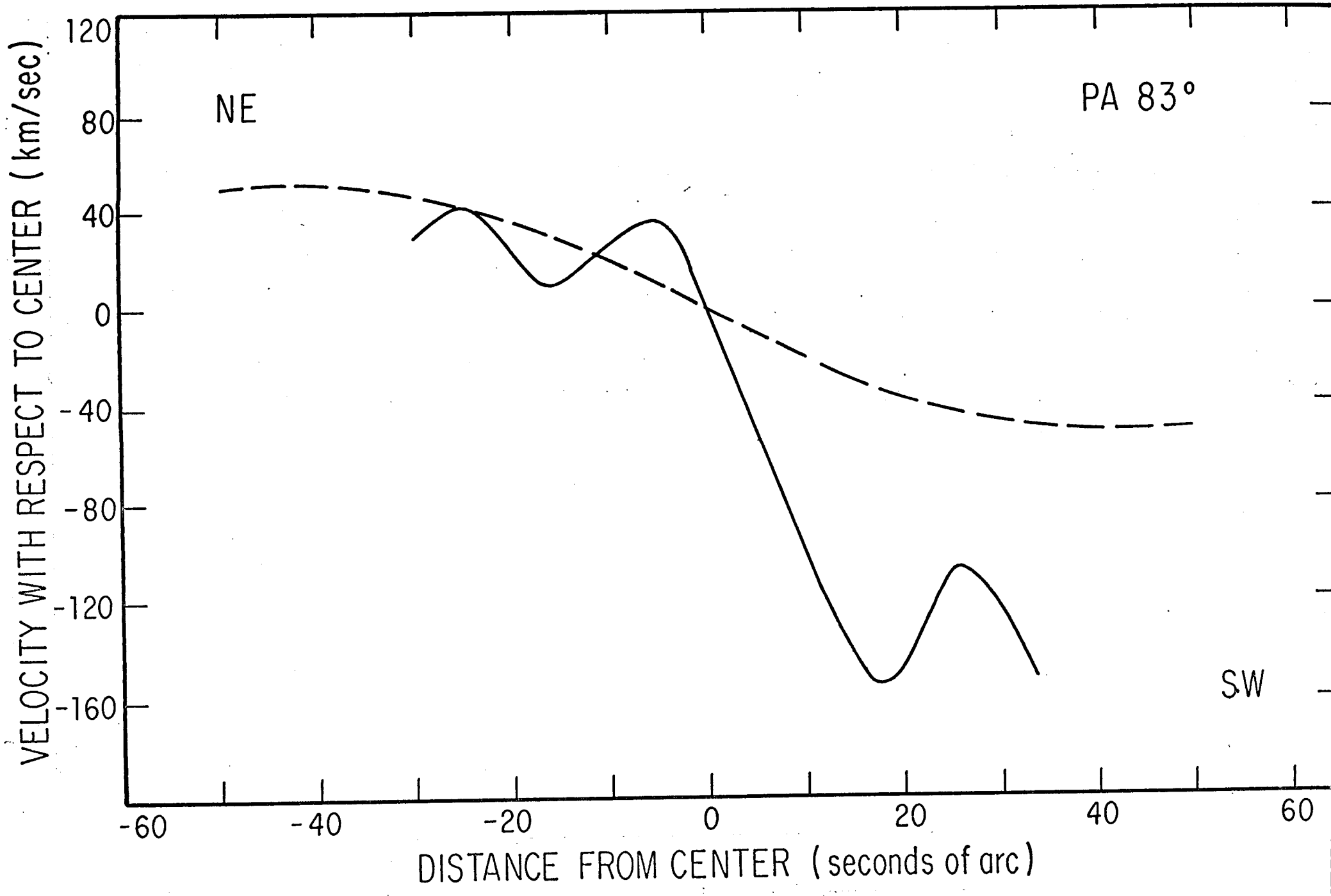
120
80
40
0
-40
-80
-120
-160
NE
PA 83°
SW
VELOCITY WITH RESPECT TO CENTER (km/sec)
-60
-40
-20
0
20
40
60
DISTANCE FROM CENTER (seconds of arc)

Fig. 2

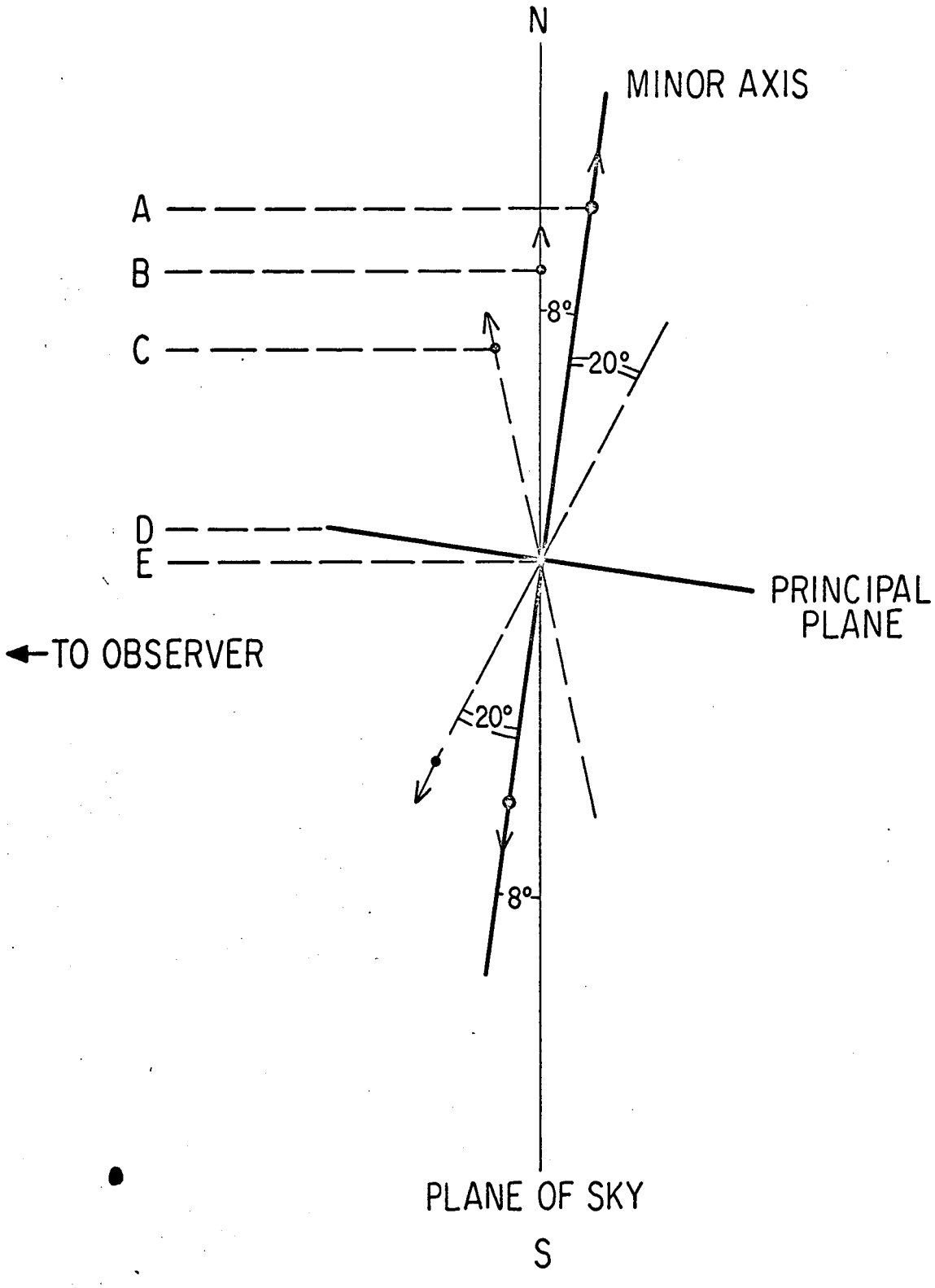
N
MINOR AXIS
A
B
C
8°
20°
D
E
PRINCIPAL
PLANE
TO OBSERVER
20°
8°
PLANE OF SKY
S

Fig. 21

Fig. 21